Teisala, H., & Butt, H.-J. (2019). Hierarchical Structures for Superhydrophobic and Superoleophobic Surfaces. *Langmuir, 35*(33), 10689-10703. doi:10.1021/acs.langmuir.8b03088.

Hierarchical structures for superhydrophobic and superoleophobic surfaces

H. Teisala* and H.-J. Butt

Hierarchical structures for superhydrophobic and superoleophobic surfaces

H. Teisala* and H.-J. Butt

Max Planck Institute for Polymer Research
Department of Physics at Interfaces
Ackermannweg 10, D-55128 Mainz, Germany

*Corresponding author: Hannu Teisala (teisala@mpip-mainz.mpg.de)

Keywords: wetting, anti-wetting, superamphiphobic, omniphobic, microstructure, nanostructure

Abstract

Many surfaces possessing robust super liquid repellency, are hierarchically structured on the nano- and micrometer scale. Several examples are found in nature such as the self-cleaning leaves of lotus plants and anisotropic, water-guiding rice leaves. Each surface design has unique properties optimized for specific wetting conditions. In this article, we review both natural and artificial hierarchical surface structures and their function in repelling liquids. We discuss different types of structures needed in various wetting situations and draw some general conclusions as a guideline for designing robust superhydrophobic and superoleophobic surfaces.

1. Introduction

Wetting of a surface is commonly characterized by measuring the contact angles between the liquid and the solid surface. On an ideally smooth, inert, and homogeneous surface the equilibrium contact angle of a drop is determined by the interfacial tension between the liquid/gas and the interfacial energies of the solid/gas and the solid/liquid interfaces, γ_{LG}, γ_{SG}, γ_{SL}, respectively, according to Young's equation (Fig. 1a):[1]

$$cos\theta = \frac{\gamma_{SG}-\gamma_{SL}}{\gamma_{LG}}. \quad (1)$$

The Young contact angle θ is sometimes referred to as a "chemical angle"[2] or "material contact angle".[3-4] On a smooth surface of a low-surface-energy material, e.g. hydrocarbons or fluorinated hydrocarbons, the maximum static water contact angle that can be achieved is of the order of ≈ 120°.[5-6] The fundamental reason for this is that the van der Waals attraction between water and any material cannot be suppressed.

Static contact angles observed on real surfaces are further influenced by contact line pinning, caused, for example, by surface roughness or heterogeneity. Basically, static contact angles are between an upper and lower limit set by the advancing and receding contact angles, respectively. The advancing contact angle θ_{adv} is the one measured when a liquid front gradually advances on the surface (Fig. 1b). A liquid can be made to advance by increasing the volume of a sessile drop, or by tilting a plate so that at a certain inclination angle the drop starts moving downhill. Correspondingly, the receding contact angle θ_{rec} is the angle measured when a liquid front gradually recedes (Fig. 1c). In general, $\theta_{adv} \geq \theta_{rec}$. The static contact angle is between advancing and receding contact angles and depends on how a drop is placed on a surface. Therefore, the advancing and the receding contact angles better describe wetting of a solid by a liquid.

Typical static contact angles measured for a water drop on a smooth, fluorinated solid are 115–120°.[7-10] The advancing and the receding contact angles are typically in the range $\theta_{adv} \approx$ 120–125° and $\theta_{rec} \approx$ 80–100°.[10-12] The difference between θ_{adv} and θ_{rec} is called contact angle hysteresis. Contact angle hysteresis is another commonly used measure to characterize wetting properties of surfaces. It is directly linked to the roll-off angle or sliding angle. The roll-off angle is determined as the angle where the drop starts to move when the substrate is inclined (Fig. 1d). When comparing

different surfaces it is important to remember that the roll-off angle depends on the drop volume. Typical drop volumes used for measuring roll-off angles are in the range of 5–15 µL.[7, 13-15]

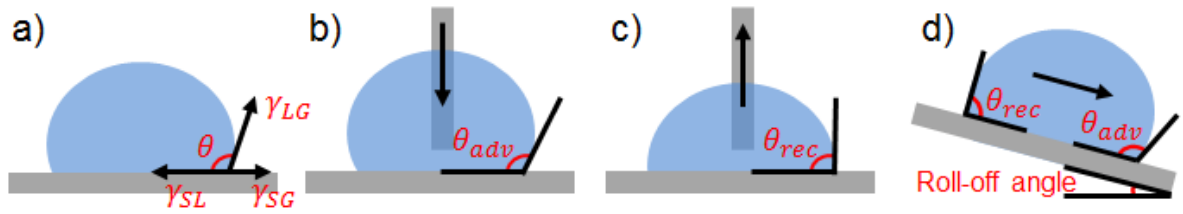

Fig. 1. Measures to define surface wettability. a) Young contact angle θ of a drop on an ideal (smooth, inert, and homogeneous) solid. b) The advancing contact angle θ_{adv} and c) the receding contact angle θ_{rec} can be measured by increasing and decreasing the drop volume, respectively. d) Alternatively, the advancing and receding contact angles can be measured by letting a drop slide/roll down an inclined solid. The roll-off angle is defined as the inclination angle at which the drop starts to move.

Much higher water repellency can be achieved on structured solids as compared to smooth solids. The surface structure needs to be such that a stable air cushion remains underneath a drop preventing wetting of the solid substrate by the liquid.[16] This wetting scenario is often referred to as the "Cassie state" or "fakir state".[2, 5, 17] Spherical drops hardly adhere to the solid and show macroscopic apparent contact angles θ_{app} exceeding 150°. Such surfaces are often called "superhydrophobic".[17-26]

Apparent contact angles are obtained by extrapolating the macroscopic shape of the drops, measured, for example, by a camera, using the Young–Laplace equation for the horizontal surface. On this scale, details of the surface structure on a < 10 µm are not visible (Fig. 2a).[15] On structured surfaces, the apparent contact angles significantly deviate from the microscopic contact angles θ on the surface. "Microscopic" refers to a length scale of > 10 nm and < 10 µm. On the 10 nm scale

surface forces come into play and again change the shape of the liquid surface near the contact line.[27] The microscopic contact angle is only visible on a microscopic scale, as demonstrated by a confocal microscope image of a superhydrophobic micropillar surface (Fig. 2b, c). Even in the case of superhydrophobic surfaces, θ cannot exceed the advancing contact angle θ_{adv} of the corresponding flat material.

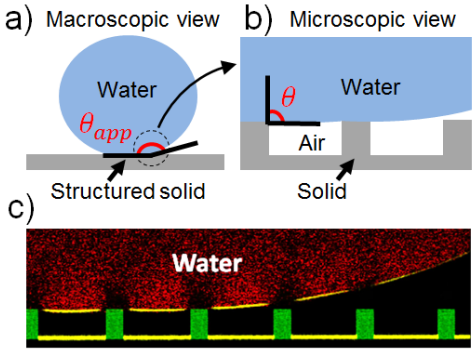

Fig. 2. Apparent and microscopic contact angle on a superhydrophobic micropillar surface. a) The apparent contact angle θ_{app} is ≥ 150° due to the air cushions within the structured surface. b) The actual microscopic contact angle θ depends on the interfacial tensions. In the case of a regular micropillar surface, θ is measured in a vertical direction with respect to the pillar wall. c) Laser scanning confocal microscope vertical image of a water drop on a superhydrophobic micropillar surface (pillar height h = 15 µm) in the Cassie state. The drop was fluorescently labelled with Alexa Fluor 488 (reproduced with permission from Ref. 15. Copyright 2016 American Physical Society).

Superhydrophobicity is commonly defined by two criteria: water should have a high apparent static contact angle ≥ 150° and a low contact angle hysteresis, or roll-off angle ≤ 10°.[17-26] The problem with this categorization is that the apparent static contact angle is an arbitrary value between θ_{adv} and θ_{rec}, whereas the roll-off angle depends on the drop volume. Therefore, we proposed to replace the two by one criterium and use the apparent *receding* contact angle. For example, if the apparent receding contact angle exceeds 150° a surface is called superhydrophobic.[15] The apparent receding

contact angle does not depend on the drop size and it determines the roll-off angle, making one parameter, not two, sufficient for definition.

Water has a high surface tension, γ_{LG} = 72.8 mN m^{-1}, which tends to keep the drop shape spherical, whereas liquids with low surface tensions, γ_{LG} = 20–40 mN m^{-1}, readily spread over solids. For many applications it is preferable to have a surface which also repels nonpolar liquids and surfactant or protein solutions. If the surface, in addition to water, shows high apparent static contact angles and low roll-off angles for nonpolar liquids, it is called superoleophobic, superamphiphobic, or super liquid-repellent.[28-29] Making the air cushions stable underneath oils and other low-surface-tension liquids is significantly more difficult than in the case of water. As soon as the air cushion collapses and the drop wets the solid in between the surface protrusions, i.e. it collapses to the "Wenzel state",[30] the super liquid-repellent properties are lost and the drop is pinned to the solid. In the Wenzel state, the apparent advancing contact angle can still exceed 150°, but the apparent receding contact angle decreases drastically.

A great number of potential applications have been proposed for super liquid-repellent surfaces. Self-cleaning is one as rolling water drops can collect the dust on the surface.[13, 24-25] Other potential applications include drag reduction,[9, 31] anti-biofouling,[32] ice repellency,[33-34] gas exchange membranes,[35-36] oil/water separation,[37-38] dropwise condensation for efficient heat transfer and fog harvesting,[39-40] manufacturing of monodisperse microparticles without consuming chemicals[41-42] or energy,[43] manipulating microdrops,[44-47] and optically transparent self-cleaning/anti-reflective coatings for wind-screens, window panes, lenses, and solar cells.[7, 48-50]

For any application, key requirements include sufficient mechanical robustness and high impalement pressure, i.e. stability of the air cushions even under high hydrostatic pressure or drop impact. When designing super liquid-repellent surfaces, we need to consider which type of surface

structure is required to optimize the low roll-off angle, mechanical stability, and high impalement pressure. Often these properties are contradictory. For example, in the case of superhydrophobic micropillar arrays a structure with a high apparent contact angle leads to low impalement pressure and vice versa.[51-52] In addition, super liquid-repellent surfaces often need to withstand harsh chemical conditions, UV light, extreme temperatures, or they need to be optically transparent.

Tuning surface structures into two or even into multiple length scales for the purpose of creating *hierarchical* surface topography is often beneficial in order to achieve the combined properties. By definition, hierarchical structures contain textures on two or more length scales.[53] Typically, hierarchical surfaces consist of a finer length scale structure on an underlying coarser length scale structure.[53-55] In this article, we review superhydrophobic and superoleophobic surfaces with respect to their hierarchical architecture. The underlying question is: What is the function of having nano- and microstructures on at least two length scales? We discuss shape and size effects of surface structures, and highlight some potential applications.

2. Super liquid-repellent surfaces

2.1. Wetting of structured surfaces

The first theory concerned with understanding the effect of roughness on wetting of solids was developed by Wenzel in 1936.[30] He introduced the roughness factor r, which is the real surface area of the rough solid divided by its projected area. To obtain the apparent contact angle θ_{app} on rough solids the cosine of the Young contact angle needs to be multiplied by this roughness factor:

$$cos\theta_{app}^{W} = r\, cos\theta. \qquad (2)$$

Accordingly, increasing real surface area enhances either hydrophilicity or hydrophobicity. Surfaces with a Young contact angle below 90° become more hydrophilic when they are rough. For surfaces with a Young contact angle above 90° the apparent contact angle increases when they are rough. Equation (2) is based on an energy minimization.

In 1944, Cassie and Baxter[16] realized that the effect described by Wenzel is not sufficient to explain very high contact angles observed for water on certain surfaces. They proposed that a layer of air can remain within a porous or rough solid underneath a liquid. They modified Wenzel's equation (equation 2) taking into account that a solid–liquid–air composite interface is sustained below the liquid. Apparent contact angles for a drop sitting on air pockets in the Cassie state can be calculated assuming the system is in global thermodynamic equilibrium:

$$cos\theta_{app}^{C} = f_1 \, cos\theta - f_2. \qquad (3)$$

Here, f_1 is the fractional area of the solid–liquid interface and f_2 the fractional area of the liquid–air interface in a plane geometrical area of unity parallel to the surface. Cassie and Baxter measured apparent advancing water contact angles > 150° on wax coated wire arrays and described their findings accordingly: "The structure of the surface thus increases the water repellency very considerably, and water drops formed on it will readily roll off."

The term "superhydrophobic" was introduced much later. To our knowledge, Busscher *et al.*[56-57] first described water-repellent surfaces as superhydrophobic in 1991. The terminology, as well as the broad interest in super liquid-repellent surfaces, started to develop rapidly after the discovery of superhydrophobic lotus leaves by Barthlott and Neinhuis[58] in 1997.

2.2. Biological surfaces

An impressive selection of surface structures with special wetting properties has evolved in nature.[58-65] Different structures are needed in different wetting environments. Well known examples include lotus leaves (Fig. 3a),[58] rose petals (Fig. 3b),[62] rice leaves (Fig. 3c),[60] and the legs of water striders.[64] Often, biological superhydrophobic surfaces have a dual scale topography: one on the 10 µm scale, one on the submicrometer scale. For example, on lotus (*Nelumbo nucifera*) leaves epidermal cells form microprotrusions. The whole surface is further covered by epicuticular wax tubules with an outer diameter of less than 200 nm.[55] Typical apparent static water contact angles > 160° and roll-off angles < 5° are measured on lotus leaves.[58, 60, 66]

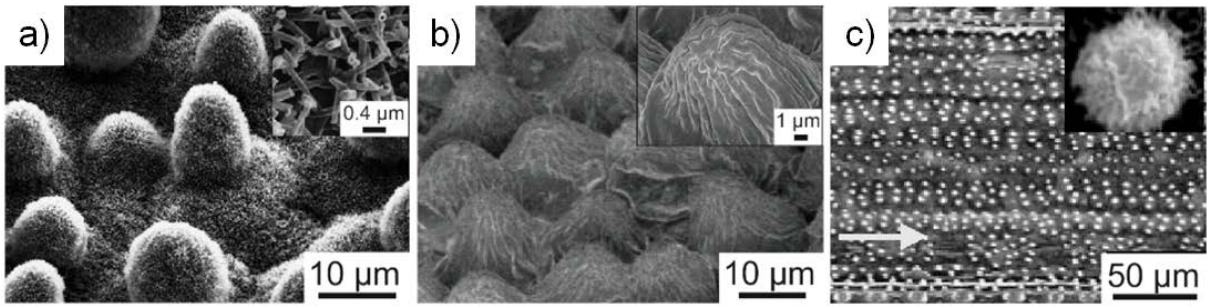

Fig. 3. Hierarchical structures of some biological surfaces. Scanning electron microscope (SEM) images of a) lotus leaf (adapted with permission from Ref. 58, Copyright 1997 Springer Nature, and from Ref. 55, Copyright 2009 The Royal Society of Chemistry), b) rose petal (adapted from Feng, L. *et al.*, *Langmuir*, 2008, *24*, 4114-4119. Copyright 2008 American Chemical Society), and c) rice leaf (adapted with permission from Ref. 60. Copyright 2002 John Wiley and Sons).

In general, the smaller the surface structures, the higher the apparent contact angle and impalement pressure.[51-52] Small structures, however, are mechanically weak. Therefore, several plants, insects and birds[2, 11, 58, 61, 63, 65, 67] rely on hierarchical surface structures which are mechanically sufficiently

strong and provide robust water repellency. Keeping dry is the key to self-cleaning of plant leaves and is crucial for insects flying in humid air conditions, e.g. termites (Fig. 4a),[65] mosquitos (Fig. 4b),[68] and cicadas (Fig. 4c),[69] or for birds when maintaining the heat insulation of their feathers.

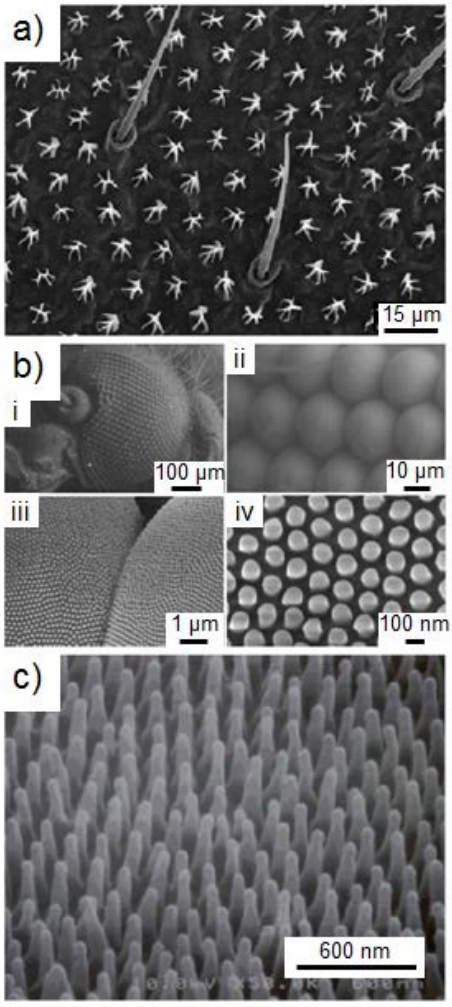

Fig. 4. Superhydrophobic surfaces of wings and eyes of some insects. SEM images of a) wing of a termite (*Nasutitermes sp.*, adapted from Watson, G. S. *et al.*, *ACS Nano* 2010, *4*, 129-136. Copyright 2010 American Chemical Society), b) eye of a mosquito at different magnifications (*C. Pipiens*, adapted with permission from Ref. 68. Copyright 2007 John Wiley and Sons), and c) wing of a cicada (*Cicada orni*, adapted from Lee, W. *et al.*, *Langmuir* 2004, *20*, 7665-7669. Copyright 2004 American Chemical Society).

Dual scale topography, however, does not always yield superhydrophobicity with a low roll-off angle. A good example is the rose petal surface (Fig. 3b).[62-63] On this petal surface the microprotrusions are covered by a folded submicrometer structure. The folded structure, conceptually different from the wax tubules of the lotus leaf, gives rise to a high solid–liquid contact area and causes drops to be pinned to the surface.[70] After rain, tiny spherical drops remaining on the surface of petals give the flower its fresh look. Apart from the aesthetic aspect, it is not clear if there is a biological reason for the surface design that gives the rose petal its specific wetting properties.

Multiple roughness scales can exist on biological surfaces. An example is the rice leaf. It has an anisotropic surface structure consisting of three different length scales: submicrometer scale structures which cover microprotrusions on the surface and macroscale grooves, ~200 μm in width and ~45 μm in height,[71] oriented in the longitudinal direction of the leaves (Fig. 3c). The anisotropic grooves can guide water shedding off the surface. Roll-off angles of water drops are ~5–10° lower in the parallel direction of the grooves than in the perpendicular direction.[60] In addition to guiding water drops, the macrogrooves enhance stability of the air cushions and protect the surface from abrasive wear. In fact, when walking in a forest or garden after rain, or on a foggy morning, we can see that many plants with long hydrophobic leaves similar to those of the rice plant, for example the Siberian Iris (Fig. 5), have anisotropic submillimeter scale protective grooves on their surfaces.

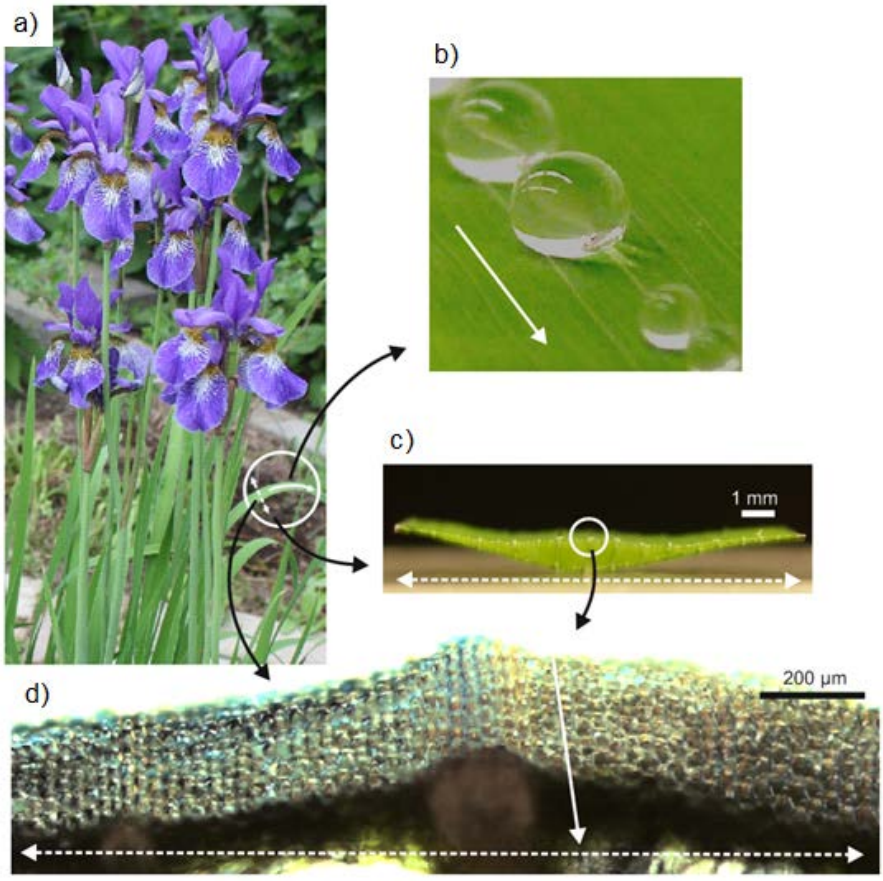

Fig. 5. Anisotropic hierarchical surface structure of leaves of the Siberian Iris (*Iris sibirica*). a) Photograph of the flowers and leaves of the plant. b) Top-view and c) cross-sectional side-view photographs showing the grooves oriented along the long, grass-like leaves. d) Cross-sectional 3D optical microscope image showing the microprotrusions and anisotropic macrogrooves of the surface. The image was compiled from several optical micrographs captured at different focal planes. White solid arrows indicate the direction of the grooves. White dotted arrows indicate orientation of the cross-sectional images.

In the case of rice leaves, the air cushions on the surface enhance photosynthesis during complete submergence.[72] Diffusion of carbon dioxide (CO_2) in air is 10^4-fold faster than in water.[72-73] Therefore, robust superhydrophobicity is an important factor for the survival of the plant. In fact, the ability of rice to enhance photosynthesis might be the answer to the question of why so many plants in nature have a hydrophobic surface structure capable of supporting air cushions. Enhanced

CO_2 uptake and photosynthesis might be among the primary reasons. Another important reason is self-cleaning.[13, 58, 74-75] However, the self-cleaning effect only applies to plants with sufficiently low roll-off angles.

Does nature always use hierarchical structures for superhydrophobic surfaces? Apparently, in most cases it does. Some insects, however, rely on one-tier structures,[59] like the wings of a cicada.[69] In contrast to insects, most plant leaves, which typically experience more mechanical stress such as the impact of rain drops or abrasive wear, have at least a two-tier surface structure.[58, 63] Exactly how much biological surfaces are limited by the fact that they have to be formed from biomaterials and by biochemical pathways poses an interesting question. Biological structures have the advantage that they can undergo self-repair after damage. In contrast, artificial materials can be stronger. Using the excellent examples of superhydrophobic structures found in nature, we can progress further by designing even better structures for liquid repellency given the advanced materials and manufacturing techniques that are now available to us.

2.3. Artificial surfaces

2.3.1. Designing hierarchical surfaces

The first works on fabrication and characterization of superhydrophobic surfaces were carried out by Wenzel[30] in 1936 and Cassie and Baxter[16] in 1944. In 1967 Dettre and Johnson[76] published their work on contact angle hysteresis on porous surfaces. In 1992 Barthlott[75] described the self-cleaning lotus-effect[58] and in 1996 Onda *et al.*[77] introduced the fractal water-repellent wax surfaces with hierarchical surface topography. Fractal surfaces are structured on all measurable length scales and are an example of another type of multiscale rough surface. On an ideal fractal surface the

roughness factor r theoretically approaches infinity. In reality, the fractal structure cannot go below molecular dimensions.

Detailed investigation of the effects of surface hierarchy on wetting was, however, postponed by almost 10 years due to lack of sufficient methods to fabricate hierarchical surfaces in a controlled manner. In 2003, Erbil *et al.*[78] used solution casting to fabricate porous superhydrophobic polypropylene surfaces with a high degree of hierarchy. The surface structure could be controlled by adjusting the solvent/nonsolvent within the solution.

In 2005, Fürstner and Barthlott[13] successfully replicated superhydrophobic hierarchical plant leaves, including the lotus leaf, by applying a molding method. They investigated the effect of a hierarchical structure on surface self-cleaning properties by using artificial fog and rain. The self-cleaning effect on hierarchical surfaces improved with the increasing velocity of impacting rain drops. The drops were able to collect dirt particles more efficiently in between the microprotrusions of the surface. Thereafter, other methods including chemical etching/electrodeposition,[8] laser etching,[79] growth of carbon nanotubes on micropatterned silicon surfaces,[80] and synthesis of raspberry-like particles[81-82] (Fig. 6) were introduced to intentionally fabricate two-tier surface structures in a controlled manner.

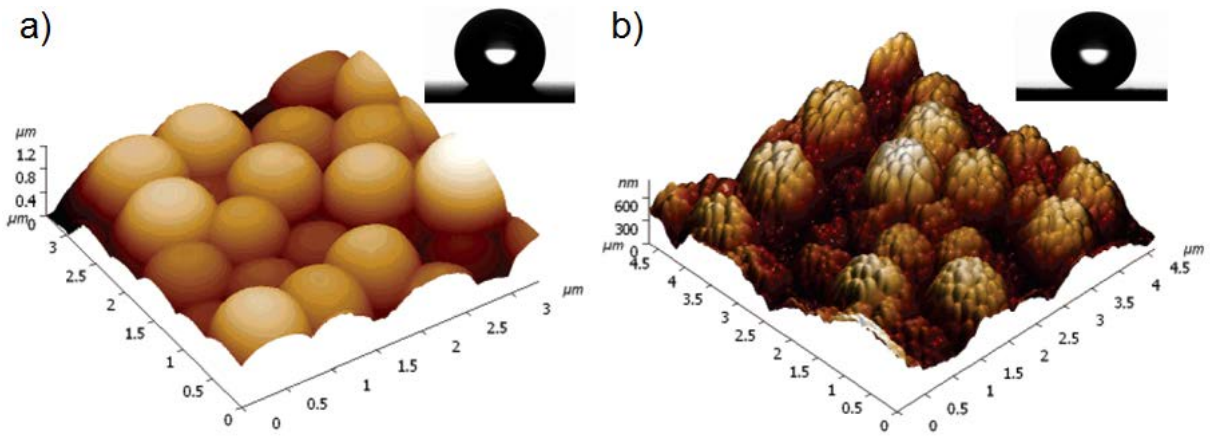

Fig. 6. Raspberry-like particle coating. Atomic force microscope (AFM) images of epoxy-based surfaces containing a) large silica particles (diameter ≈ 700 nm) and b) the large and small silica particles (diameter ≈ 70 nm). The surfaces were coated with polydimethylsiloxane (PDMS) to render them hydrophobic. Insets: shape of 5 µL water drops on the respective surfaces. Adapted from Ming, W. *et al.*, *Nano Lett.* 2005, *5*, 2298-2301. Copyright 2005 American Chemical Society.

2.3.2. Stability of the Cassie state

Stability of the Cassie state is one of the key criteria when designing super liquid-repellent surfaces. Given this, current research has concentrated on improving our understanding of wetting states and wetting transitions on rough surfaces. Energy balance calculations indicate that the existence of air cushions on a superhydrophobic surface is thermodynamically favorable, i.e. the drop has lower energy in the Cassie state than in the Wenzel state, if $\theta_{app}^{C} < \theta_{app}^{W}$ and vice versa.[6, 83-84] Depending on morphology and chemical composition of the surface, the drop can have several preferable, metastable wetting states where it reaches its local minimum energy.[83-85] The static shape of the drop on such surfaces, therefore, depends on how it was formed or deposited on the surface. Basically, the Cassie state is often attained when a drop is placed on a superhydrophobic surface, even though the Wenzel state would be thermodynamically more favorable.

The change from one wetting state to another requires work, i.e. the energy barrier separating the two wetting states needs to be overcome.[6, 12, 84, 86-87] It is reasonable to ask how we can maximize this energy barrier and how we can prevent a transition from the superhydrophobic Cassie state to the fully wetted Wenzel state. Thermodynamic calculations suggest that hierarchical structures can make the Cassie state energetically more favorable as compared to the Wenzel state.[54, 83, 88-90] Maximizing the energy barrier becomes critically important in humid conditions where condensing

drops grow on the surface, or when millimeter-sized rain drops impact the surface. Maximizing the microscopic θ_{adv} and θ_{rec} of the material helps in sustaining the Cassie state.

2.3.3. Breakdown of the Cassie state

Consider a water drop resting on an air cushion on a structured surface. In a static situation the curvature of the liquid–air interface is determined by the radius of the drop. Thus, the liquid–air interface is also curved between the surface protrusions. The pressure change over the curved liquid interface is given by the Young–Laplace equation

$$\Delta P = \gamma_{LG}\left(\frac{1}{r_1}+\frac{1}{r_2}\right), \tag{4}$$

where r_1 and r_2 are the principal radii describing the meniscus curvature. For a spherical interface we get

$$\Delta P = 2\gamma_{LG}/r. \tag{5}$$

Capillary pressure generated within the hydrophobic surface structures prevents the drop from penetrating the structure of the solid. For a surface with a simple circular pore geometry with pore diameter d, the radius of curvature of the liquid interface within the pore thus is $r = d/2cos\theta$.[91] Inserting this expression in equation 5 and selecting $\theta = \theta_{adv}$ we get the upper limit for the capillary pressure before water enters the pore

$$P_C = -4\gamma_{LG}cos\theta_{adv}/d. \tag{6}$$

In equation 6 we immediately see that in addition to decreasing pore diameter, the water-entry-pressure increases with increasing surface tension and advancing contact angle of the liquid on the given solid. Surface structures which are composed of nanopores can generate a high water-entry-pressure to provide robust repellency against liquid impalement.[92]

For a cylindrical pillar array the capillary pressure is given by[52]

$$P_C(1-\emptyset) = -\frac{2\pi a \gamma_{LG}}{A} cos\theta_{adv} \quad (7)$$

where a is the pillar radius, A is the area occupied by a single pillar at the array, and $\emptyset = \pi a^2/A$ is the projected solid area fraction of the pillars at the surface.

Increasing internal pressure of the drop, e.g. by drop impact, squeezing, increasing the hydrostatic pressure, or decreasing the drop size, can force the liquid to penetrate from the Cassie state to the Wenzel state. If the pressure applied by the liquid to the surface exceeds the water-entry-pressure, the contact angle of the liquid at the protrusion walls reaches θ_{adv} and the three phase contact line starts to slide down the walls (Fig. 7a and Fig. 8).[4, 93] In addition, if the surface protrusions are not sufficiently high, the liquid sags and touches the substrate (Fig. 7b).[93] In this case, the drooping liquid makes contact with the substrate in between the surface protrusions before it reaches θ_{adv}. After the so-called Cassie-to-Wenzel transition the solid underneath the liquid is wetted entirely and the drop is pinned to the surface.

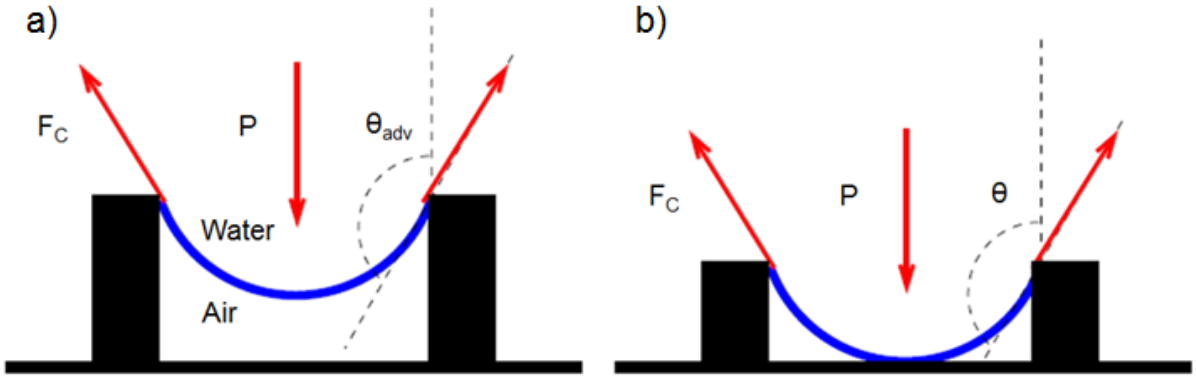

Fig. 7. Pressure driven transition from the Cassie to Wenzel state. Sketches of a) the "sliding" and b) "sagging" scenario. F_C denotes the capillary force balancing the applied pressure P. Adapted with permission from Ref. 93. Copyright 2006 EDP Sciences.

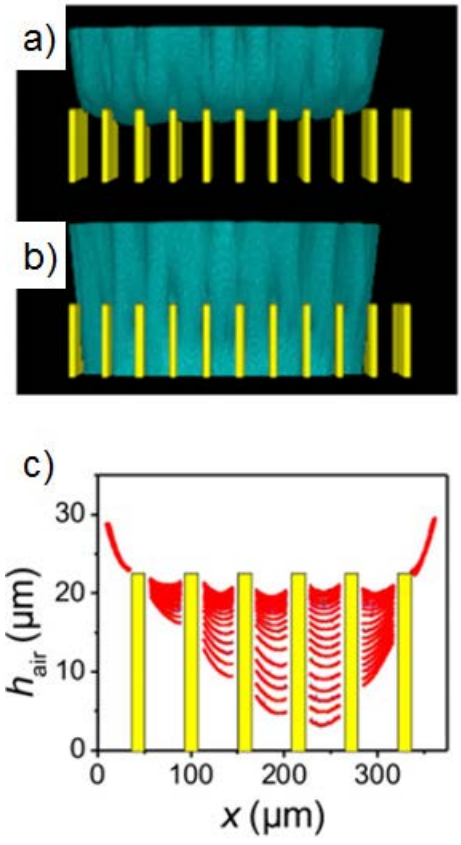

Fig. 8. Monitoring Cassie-to-Wenzel transition via "sliding". a) 3D laser scanning confocal microscope image of a fluorescently labeled water drop on an array of micropillars. While the drop evaporates and decreases in radius, its Laplace pressure increases according to equation 5. b) When the Laplace pressure exceeds the critical water-entry-pressure the Cassie state collapses. c) Profiles

of the thickness of the air cushion measured during the evaporation along a diagonal and passing through the center of the drop. Adapted with permission from Ref. 4.

2.3.4. Recovery of the Cassie state

Preventing Cassie-to-Wenzel transition can be a challenge when, for example, drops impact the surface at high-velocity, or when the surface is immersed in a liquid at high hydrostatic pressure. This raises the question as to whether the Cassie state recovers spontaneously after the pressure is released again. Molecular simulations indicate that recovery of the Cassie state is possible on nanostructured surfaces due to density fluctuations of water[94] or due to surface geometry,[95-96] for example, on cone-shaped structure. To our knowledge, however, experimental validation of the spontaneous recovery of the Cassie state has not yet been achieved. Typically, excess energy is needed to trigger the Wenzel-to-Cassie transition – even if the Cassie state were energetically favorable over the Wenzel state. The reason for this is that spontaneous transition is prevented by the large energy barriers and contact angle hysteresis, i.e. the receding contact angle of the material θ_{rec} is usually lower than 90°.

On a hierarchical surface structure composed of microstructures covered by nanostructures, different wetting states can exist (Fig. 9). If the pressure exceeds the capillary pressure generated within the microstructures and the liquid is partially impaled, the nanostructures still prevent a transition to a full Wenzel state. Spontaneous transition to the "micro-Cassie" state (Fig. 9a) from the "nano-Cassie" state (Fig. 9b) is possible after external pressure is released.[97] The reason for this is the low energy barrier for the transition.[98] The nano-Cassie state still has a receding contact angle much higher than 90°. When the applied pressure exceeds the water-entry-pressure within the nanostructures, the Wenzel state (Fig. 9c) is stable and the system will not spontaneously go back to the Cassie state.

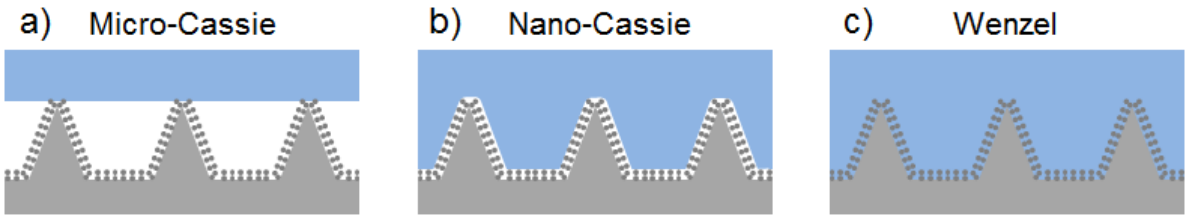

Fig. 9. Possible wetting states on hierarchical surfaces. Characteristic for the Cassie wetting state is formation of a composite solid–liquid–air interface. a) Micro-Cassie state where the air cushions are preserved in both the micro- and nanostructures of the surface, e.g. wetting state of large water drops resting on a lotus leaf. b) Nano-Cassie state where the liquid fills the microcavities while the nanostructures hold the air cushions, e.g. rain drops impacting a lotus leaf.[13] c) Fully wetted Wenzel state where air cushions do not exist and a drop is pinned to the surface, e.g. prolonged condensation of water on a lotus leaf.[66]

2.3.5. Superoleophobic surfaces

In 1997, Tsujii *et al.*[99] managed to fabricate a fractal, fluorinated surface which was not only superhydrophobic, but in addition superoleophobic. Drops of rapeseed oil showed a high apparent contact angle of 150° and easily rolled off at a low tilting angle. In 2000, Herminghaus[100] described the principle of superoleophobicity where overhang structures support the liquid interface. Some 7 years later, Tuteja *et al.*[101] designed superoleophobic mushroom-like micropillar surfaces that are capable of repelling low-surface-tension and non-polar liquids.

The analogy of wetting on a superoleophobic surface is similar to that on a superhydrophobic surface: the liquid hanging between the surface protrusions cannot have a higher microscopic contact angle θ than the intrinsic wettability of the material defined by θ_{adv}.[102-104] To fulfill this criterion, a necessary design principle for superoleophobic surfaces is a re-entrant, inward curved

morphology due to the fact that for any oil θ_{adv} < 90°. To repel liquids of very low surface tension γ_{LG} < 20 mN m^{-1}, for example fluoroalkanes, doubly re-entrant surface structure may be required.[105] Re-entrant morphology can be realized by well-defined "micro-hoodoo" pillars (Fig. 10),[101, 105] by depositing nanofilaments[36, 106] (Fig. 11a), or nanoparticles[7, 49, 107] (Fig. 11b). Another method of producing superoleophobic surfaces is to pattern micro-/submicrostructures with nanopores (Fig. 11c).[108-109]

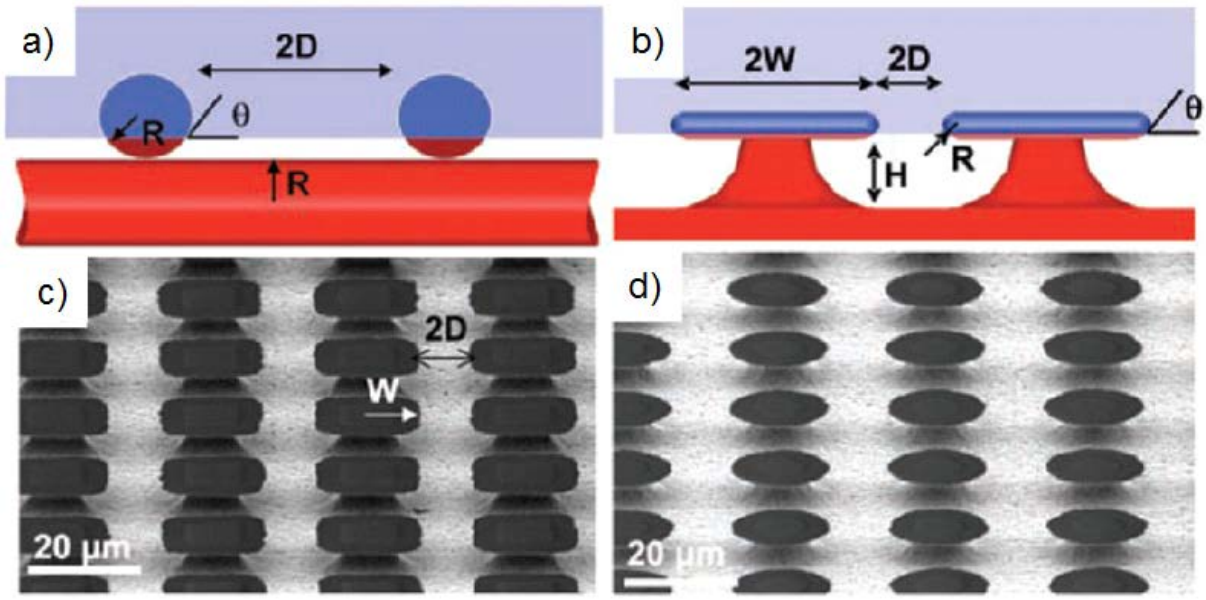

Fig. 10. Wetting of re-entrant surface structures. Figures highlighting formation of a solid–liquid–air composite interface on oil-repellent a) fiber and b) "micro-hoodoo" surfaces. Blue color indicates wetted area and red non-wetted area when the liquid has θ < 90°. SEM images of c) square top and d) circular top re-entrant micropillars. Reproduced with permission from Ref. 101. Copyright 2007 The American Association for the Advancement of Science.

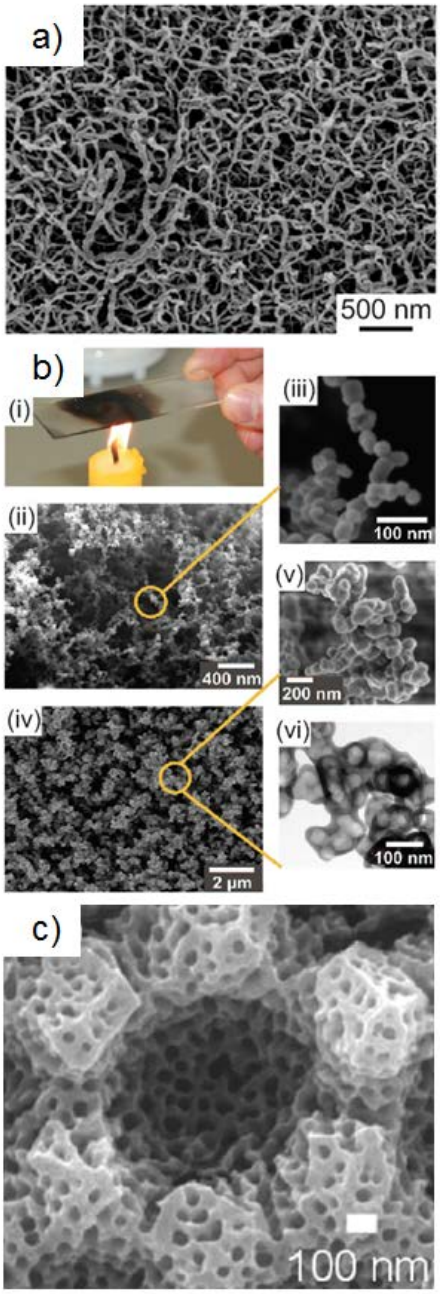

Fig. 11. Randomly structured surfaces with re-entrant curvature. a) SEM image of silicone nanofilament coating (adapted with permission from Ref. 36. Copyright 2016 John Wiley and Sons). b) Fabrication of a soot templated superamphiphobic coating: (i) deposition of candle soot particles, (ii, iii) SEM images of resulting soot morphology, (iv, v) SEM and (vi) transmission electron microscope images of the coating after growing a 20-nm-thick silica shell and calcinating in an oven (reproduced with permission from Ref. 107. Copyright 2011 The American Association for the Advancement of Science). c) SEM image of submicrostructures decorated with nanopores

(reproduced from Fujii, T. *et al.*, *J. Phys. Chem. C* 2012, *116*, 23308-23314. Copyright 2012 American Chemical Society).

2.4. Different surface structures for different wetting situations

2.4.1. Mechanical robustness

One reason for developing hierarchical surfaces containing nano-, micro-, and even macroscale structures is enhanced mechanical robustness. Hierarchical structures prevent mechanical damage in two ways. First, micro- and macroscale protrusions are stronger than submicro- and nanostructures. Secondly, the fragile submicro- and nanostructures are shielded in between the surface protrusions as only the top parts of the protrusions get damaged by mechanical contact (Fig. 12).[110-112]

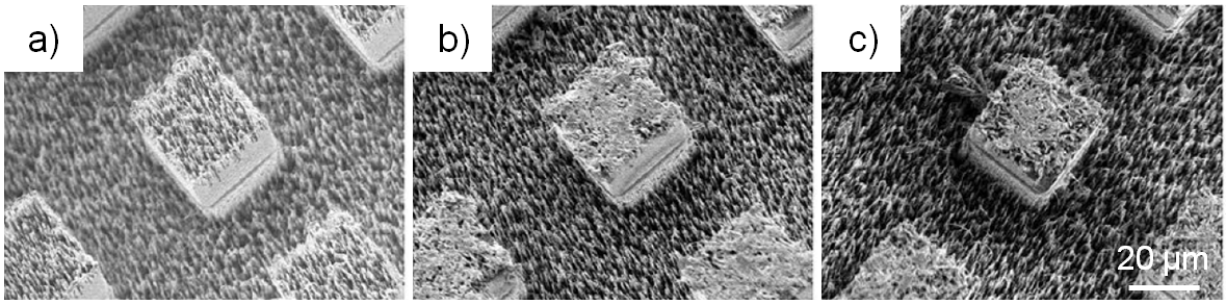

Fig. 12. SEM images of nanograss-covered microposts. a) Before an abrasion wear test, b) after the wear test with 1 N, and c) after the wear test with 20 N. Adapted from Groten, J. and Rühe, J., *Langmuir* 2013, *29*, 3765-3772. Copyright 2012 American Chemical Society.

Recovery after mechanical damage remains an issue in the case of artificial super liquid-repellent surfaces. Therefore, improving mechanical durability of the surfaces as far as possible is of crucial importance. It has been shown that fabrics coated with the right combinations of elastic and rigid

materials can yield a remarkably durable state of superhydrophobicity.[113-114] Such surfaces contain three crucial elements for mechanical stability: hierarchical structures, deformability, and hardness.

2.4.2. Drop adhesion

Minimizing the solid–liquid interactions is a prerequisite in achieving a high apparent receding contact angle, low vertical and lateral adhesion, and low friction of a moving drop on a surface.[11, 31, 115] Gao *et al*.[11] showed that a lateral force less than 10 μN is required to move a water drop on a superhydrophobic nanofilament coating (Fig. 13). The overall solid–liquid contact area and adhesion on a super liquid-repellent surface can be reduced by decreasing the size of the surface structures, or by increasing the distance between the protrusions. Increasing the distance yields low liquid-entry-pressure. Therefore, reducing the dimensions of the surface structure down to submicrometer- or even nanoscale is often a more appropriate choice.[51-52]

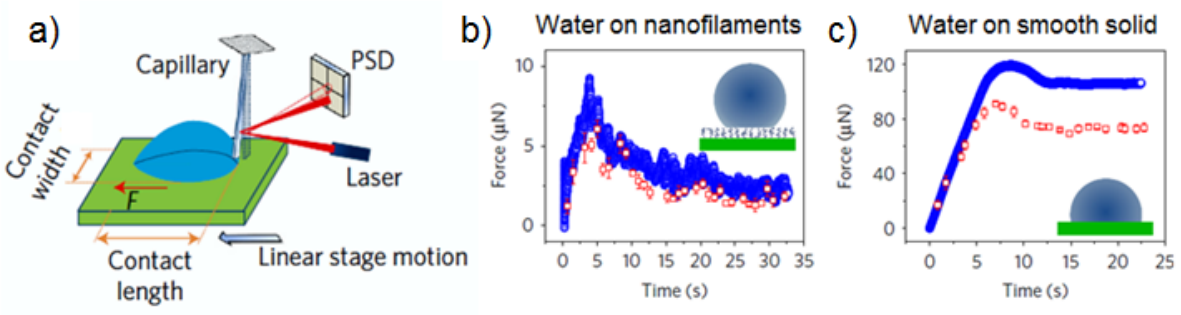

Fig. 13. Solid–liquid friction force measurement. a) Schematics of the setup. A laser beam is reflected from a capillary to a position-sensitive detector (PSD). The contact width and length between the drop of liquid and the solid surface are monitored by cameras (not shown). Measured (blue circles) and calculated (red squares) friction forces on b) superhydrophobic fluorinated nanofilaments and c) smooth fluorinated silicon wafer. Adapted with permission from Ref. 11. Copyright 2017 Springer Nature.

Hierarchical surface structures are an efficient way of reducing drop adhesion, because the microstructures entrap large pockets of air and thus reduce the solid–liquid interaction. With water, however, it is not always necessary to introduce a second length scale, provided that improving mechanical robustness is not important, e.g. in the case of the eyes and wings of some insects. The drop adhesion can be efficiently reduced even with a one-tier surface structure on the submicrometer scale because of the high surface tension of water. High apparent receding contact angles > 150° and low roll-off angles < 1° for water can be achieved even with one-tier surface topography.[9-10, 55, 116]

On superamphiphobic surfaces the requirements for surface morphology are stricter as compared to superhydrophobic surfaces. Therefore, reducing solid–liquid interaction by hierarchical structures capable of trapping large air cushions is often beneficial. As an example, a superamphiphobic flame-sprayed nanoparticle coating with a high degree of hierarchy displayed an apparent receding contact angle > 150° and low roll-off angle even below 1° for 10 µL drops of *n*-hexadecane, Fig. 14.[7]

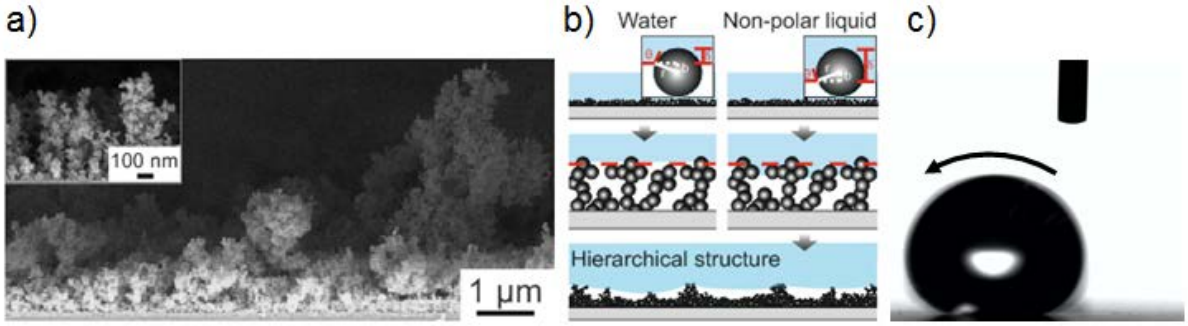

Fig. 14. Superamphiphobic surface with high degree of hierarchy. a) SEM side-view image showing morphology of TiO_2/SiO_2 nanoparticle coating fabricated by liquid flame spray (LFS). Primary particle size is 10–20 nm. The highest aggregates of particles are at least 7 µm high, resulting in a high surface hierarchy. b) Illustration how re-entrant fluorinated nanostructures together with high hierarchy of the surface yield a low solid–liquid contact area even for non-polar liquids. 10 µL

drops of water and c) *n*-hexadecane, γ_{LG} = 27.5 mN m^{-1}, roll off the surface at inclination angles < 1°. Adapted with permission from Ref. 7. Copyright 2018 John Wiley and Sons.

2.4.3. Drop impact

When a drop hits a structured surface, such as falling rain drops, the pressure P created by the impact forces the liquid to penetrate the structure. Capillary pressure P_C generated within the surface texture acts in the opposite direction preventing the liquid from penetrating the structure. Thus, liquid is assumed to penetrate the structure in the Wenzel state if $P > P_C$.[3, 93, 117]

The wetting pressure P can be estimated by calculating the dynamic pressure P_D[3, 93] for the impacting drop. The dynamic pressure is an estimate for the average pressure generated within the drop impact. It does not take into account the spherical shape of the drop and pressure distribution over the impacted area.

As an example, consider a spherical drop impacting a surface. At the initial stage of the impact only a tiny area of the drop contacts the surface due to the curvature of the liquid. The drop starts to deform. Due to impact and spherical shape of the drop, compressional waves are progressively generated within the drop. In addition, the kinetic energy of the drop is dissipated in surface energy and spreading in a lateral direction. As a result, the maximal pressure is not evenly distributed underneath the drop.

The mean force required to stop the impacting drop is

$$\overline{F} = \frac{p}{2R/v} = \frac{mv^2}{2R} = \frac{4\pi R^3 \rho v^2}{6R} = \frac{2}{3}\pi R^2 \rho v^2. \quad (8)$$

Here, p is the momentum, R the radius, v the velocity, m the mass, and ρ the density of the drop.

The mean dynamic pressure is of the order of

$$\overline{P}_D = \frac{\overline{F}}{\pi R^2} = \frac{2}{3}\rho v^2. \quad (9)$$

The pressure in the center of an impacting drop is higher than at the periphery where the drop spreads. As a result, partial liquid entry is often observed in the center, Fig. 15.[92]

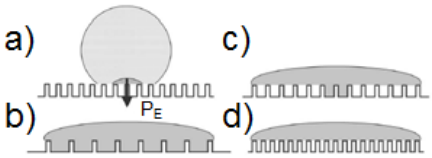

Fig. 15. Different wetting states of impinging drops. a) Effective maximal pressure P_E generated during the contact stage and dynamic pressure P_D during the spreading stage. Capillary pressure P_C resisting the liquid impalement increases with decreasing pillar spacing. Different wetting states can result from constant impact velocity if pillar spacing is varied: b) total wetting state (P_E>P_D>P_C); c) partial wetting state (P_E>P_C>P_D); d) total non-wetting state (P_C>P_E>P_D). Adapted with permission from Ref. 92. Copyright 2009 AIP Publishing.

Impacting drops on hierarchical surfaces often penetrate the surface microstructure partially or completely, still leaving the nanostructure in the Cassie state. This transition from micro-Cassie to nano-Cassie is often reversible due to the low kinetic barrier for the transition, as depicted in Fig. 9. The microstructure already dissipates part of the kinetic energy so that the nanostructures only need to support the remaining energy of the impacting drop. An example is the self-cleaning effect of lotus leaves caused by impacting rain drops.[13] Thus, in addition to mechanical durability, the

microstructure – on biological hierarchical surfaces often in the order of 10 µm – provides resistance against liquid-entry within drop impact.

In addition, hierarchical structures influence the shape of rebounding drops and their contact time with the surface. Liu *et al.*[97] showed that reversible transition from micro-Cassie to nano-Cassie occurs within drop impact on the appropriate design of tapered submillimeter-scale posts covered with nanostructures (Fig. 16a). As a result, the drop bounces off the surface in the shape of a pancake (Fig. 16b). The drop is lifted up right after emptying the capillaries which the liquid penetrated during impact. Take-off occurs just after recovering the micro-Cassie state. This happens close to maximum spreading of the drop. As a result, the contact time of the drop is fourfold shorter as compared to a nanostructured surface where the drop needs to retract before leaving the surface (Fig. 16c).

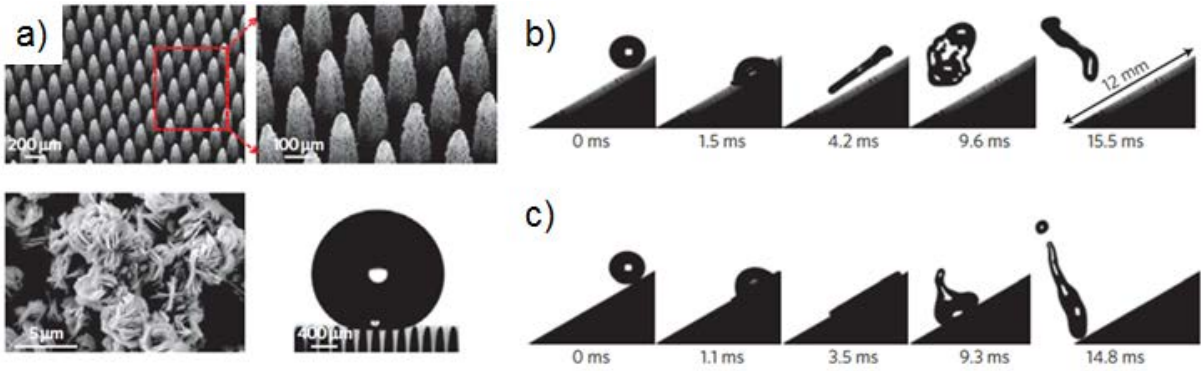

Fig. 16. Hierarchical surface structures reducing contact time of impacting drops. a) SEM images of tapered copper microstructures covered with nanotextures. A photograph of a water drop resting on the surface with an apparent contact angle > 165° and contact angle hysteresis < 2°. b) A water drop impacting the hierarchical surface experiences "pancake bouncing" due to reversible capillary filling of the surface microstructures during impact, which allows rapid departure of the drop from the surface as compared to c) conventional impact dynamics of a drop on only a nanostructured surface. Reproduced with permission from Ref. 97. Copyright 2014 Springer Nature.

Contact time during drop impact controls the mass, momentum, and energy exchange between the drop and surface.[118-119] Therefore, it is often beneficial to reduce it. A common reason for aiming at short contact times is to achieve the reduction of ice formation on surfaces.[119-121] When a supercooled water drop hits a surface, the surface provides many nucleation sites and the water freezes. Despite the connection between the contact time and potential reduction of freezing, we are not currently aware of any experimental evidence proving that this hypothesis is correct.

Another approach to reduce the contact time of impacting drops is to use anisotropic hierarchical surface structures on the macroscopic scale. Bird *et al.*[119] showed that macrostructures of the order of ~100 µm can redistribute mass of the drop, which induces splitting of the impacting drop. They demonstrated a 37% reduction in the contact time of impacting drops on a superhydrophobic surface with macrostructures as compared to a superhydrophobic surface without macrostructures.

While hierarchical surface structures are beneficial in drop impact – to prevent transition to the Wenzel state and to reduce contact time of impacting drops – they do not prevent impalement in submerged environments where the wetting transition is driven by hydrostatic pressure. There, the pressure experienced by the surface is uniform, also in between the microstructures. Thus, a multi-tier surface structure does not improve resistance against impalement. The liquid-entry-pressure is determined by the submicro- or nanostructures on the surface.

2.4.4. Guided liquid transport

Guided liquid transport can be achieved by anisotropic hierarchical structures. For example, aligned structures on biological surfaces often serve the purpose of allowing water to run off in a specific direction.[60, 63] Examples include the submillimeter scale longitudinal features on rice leaves (*Oryza*

sativa, Fig. 3c)[60] and the scale-like structures on butterfly wings (*Morpho aega*),[67] which only allow water to roll in one direction – away from the body of the insect.

Mertaniemi *et al.*[122] demonstrated how the transport of water drops could be guided on a macrostructured artificial surface: the drops precisely followed a 300 µm deep track made on a superhydrophobic surface. The drop moving on the track is pressed down by gravity and is supported by the track edges (Fig. 17, upper row).

Zhao *et al.*[14] fabricated anisotropic, grooved superamphiphobic surfaces by photolithography followed by deep reactive ion etching. 10 µL drops of *n*-hexadecane rolled off the surface at the tilt angle of 4° in the parallel direction and at an angle of 34° in the perpendicular direction to the re-entrant grooves. In the parallel direction of the grooves the drop can smoothly advance. In contrast, in the perpendicular direction there is a barrier for the drop motion due to the repeated pinning and depinning events as the liquid advances over the air gaps at the grooves (Fig. 17, lower row).

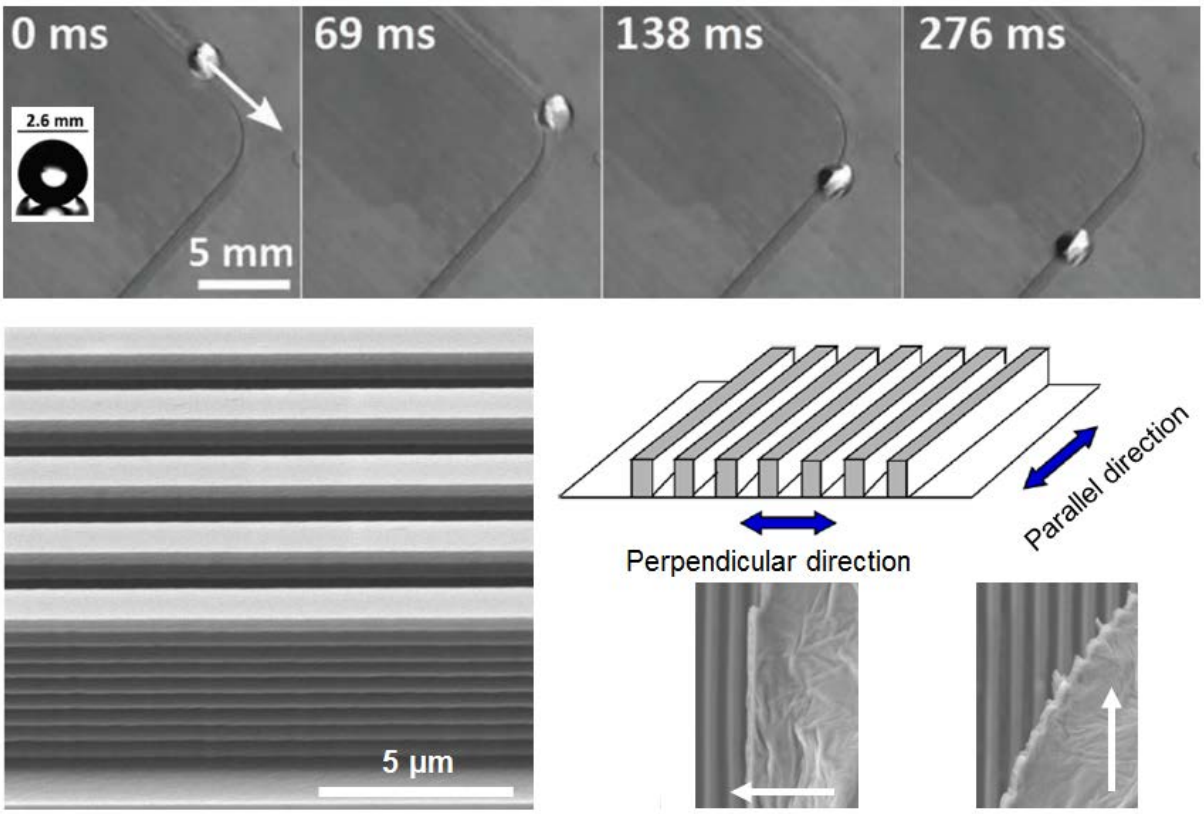

Fig. 17. Guided liquid transport on a superhydrophobic track and a surface with linear microgrooves. Upper row: a sequence of images showing a 10 µL water drop guided by a superhydrophobic copper track. Track width is 1 mm. Inset: a 2.6 mm wide water drop supported by a 1.6 mm wide groove. Reproduced with permission from Ref. 122. Copyright 2011 John Wiley and Sons. Lower row, left: a SEM image of a grooved re-entrant textured surface. Lower row, right: schematic for the grooved structure and SEM images of the contact lines of sliding ink drops in the perpendicular and parallel directions of the grooves. Adapted from Zhao, H. and Law, K. Y., *Langmuir* 2012, *28*, 11812-11818. Copyright 2012 American Chemical Society.

2.4.5. Condensation

Supersaturated humidity can induce Cassie-to-Wenzel transitions and loss of superhydrophobicity due to condensing drops on the surface structures. One-tier microstructured surfaces are particularly prone to losing their hydrophobic properties when water drops condense on the structure walls.

Scaling down the structure size can hinder wetting of superhydrophobic surfaces in humid conditions, because suitable design of submicro- or nanoscale structures induces self-propelled jumping of drops off the surface.[10, 116] The self-removal of drops is driven by excess surface energy released and transformed into kinetic energy upon coalescence of the drops.[40]

Suitable design of hierarchy can further facilitate the departure of condensing drops from multi-tier structured surfaces as compared to just nanostructured surfaces.[123] Both conical[124] or pyramidical[125] microstructures covered with nanostructures serve the purpose. Chen *et al.*[125] demonstrated that hierarchical surface structure with micro-pyramid architecture increased the self-removal volume of water by ~450% as compared to a superhydrophobic surface with only nanotextures. The enhanced removal of water from the hierarchical surface was associated with the self-propelled jumping of drops and their random sweeping of other drops from the surface.

Although self-propelled removal of condensed drops has been demonstrated on some artificial hierarchical surfaces, condensing water on a lotus leaf was shown to pin to the surface.[66] One reason could be that biological surfaces rely on waxy materials with a lower degree of intrinsic hydrophobicity as compared to artificial, fluorinated materials. Furthermore, preventing condensation is not a crucial property for lotus leaves as they are not exposed to freezing temperatures in their natural habitat. Some other biological surfaces like that of Lady's Mantle (*Alchemilla vulgaris L.*)[61] and the wings of some termites (e.g. *Nasutitermes sp.*, Fig. 4a)[65] rely on their hierarchical surface design with hairy structures to remove condensed microdrops.

Despite the benefits of surface hierarchy in preventing condensation wetting, some insects rely on just one-tier submicrometer scale structures to prevent wetting when flying in fog (Fig. 4). In fact, Mouterde *et al.*[126] showed that drops even smaller than 2 μm could be expelled from a surface composed of nanometer scale cones mimicking the wings of cicada. Water adhesion on the

nanocone surface remained drastically lower at humid conditions as compared to cylindrical nanopillars of comparable size (Fig. 18). The geometry of nanocones influences adhesion of condensed water in two ways: at the bottom of the cones water condensation is impeded due to the vanishing gap between the cones; and in addition Laplace pressure constantly forces condensed drops out of the structure. It remains to be shown whether a hierarchical surface composed of conical or pyramidical microstructures covered with such nanocones could further improve removal of condensing water. Artificial surfaces able to efficiently remove condensed water are of interest in designing surfaces to enhance heat transfer,[123, 127] to harvest water from humid air,[116] and to delay frost growth.[128]

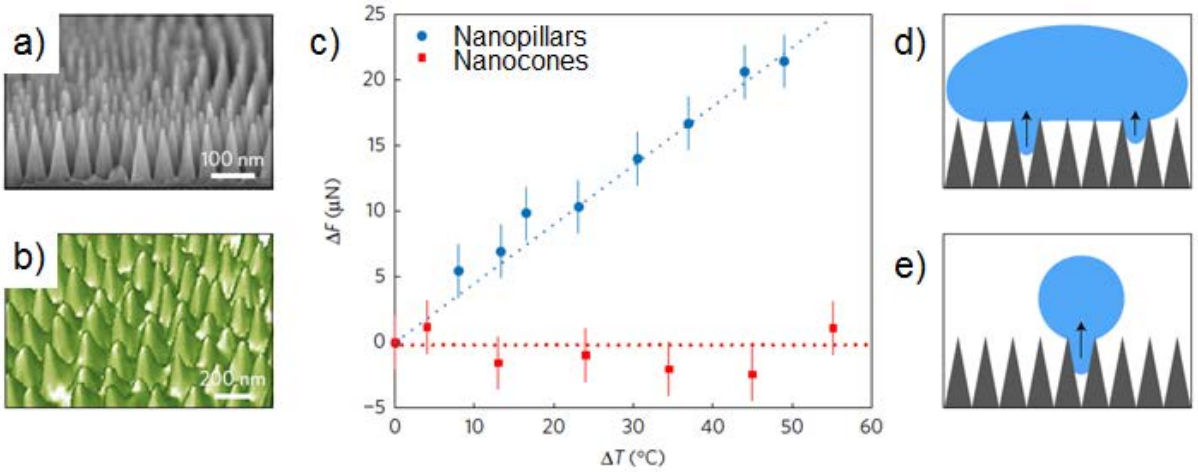

Fig. 18. Adhesion of hot drops on nanopillars and on nanocones. a) SEM image of the nanocones mimicked from b) the wings of cicada (*Psaltoda claripennis*, atomic force microscope image). c) Adhesion force ΔF due to condensation as a function of temperature difference ΔT between water and substrate. d, e) Sketches showing the effect of geometry: Laplace pressure drives condensed water out of the surface structure. Adapted with permission from Ref. 126. Copyright 2017 Springer Nature.

2.4.6. Selective permeability

One potential field of application for super liquid-repellent surfaces is the selective permeation of fluids through a membrane. In this case, there are naturally two or more length scales involved. The liquid-repellent coating forms a structure on the nano- and/or micrometer scale and the membrane itself adds another structure level on the macrometer scale. One fluid can permeate through the membrane while the other is repelled. A common example of this is the separation of oil from water through a membrane with superhydrophobic and superoleophilic properties.[129] Other relevant examples are oxidation of blood (γ_{LG} = 47 mN m^{-1})[35] and carbon dioxide capture by aqueous amine solutions[36] (Fig. 19) through superamphiphobic membranes. These membranes prevent low-surface-tension liquids from permeating, while allowing a high rate of gas exchange through the membrane.

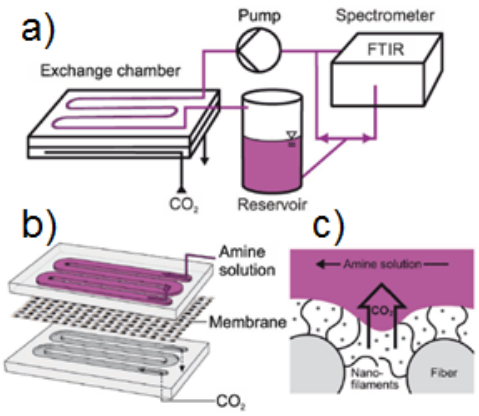

Fig. 19. Carbon dioxide captured through a superamphiphobic membrane. a) Sketch of the experimental setup to quantify carbon dioxide uptake. b) Structure of the exchange chamber. c) Schematic of carbon dioxide captured through nanofilament coated polyester membrane. Reproduced with permission from Ref. 36. Copyright 2016 John Wiley and Sons.

2.4.7. Structural color and optical transparency

Often natural superhydrophobic surfaces display beautiful colors. The reason is that structures needed for repelling water selectively reflect light and can cause interference effects if the size of the surface structure matches the wavelength of light.[130] For visible light, the generation of structural colors would require surface structures to be ~200–700 nm in size, which is often the case with natural superhydrophobic surfaces. Examples of biological surfaces combining fascinating anti-wetting properties and colors include rose petals, butterflies, beetles, and the feathers of many birds such as mallards and peacocks.[131]

In contrast, many potential applications of super liquid-repellent surfaces, such as anti-wetting and self-cleaning windows and lenses, require optical transparency. Good transparency requires surface structures smaller than the wavelength of visible light. Therefore, when optical transparency needs to be combined with surface hierarchy, it might be appropriate to avoid using microstructures that can partially reflect the light and thus reduce transparency. Instead, the required hierarchical surface topography can be created, for example, via particle aggregates where the primary particle size remains well below the wavelength of light (Fig. 20).[7, 107]

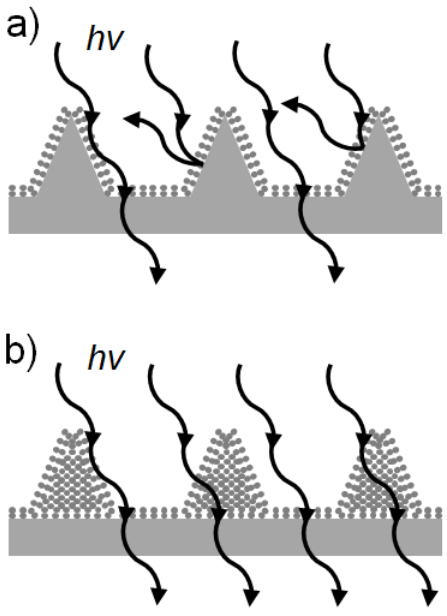

Fig. 20. Light transmittance on hierarchically structured surfaces. a) Light is partially reflected from a surface containing nano- and microstructures. b) Light is transmitted through a nanostructured surface with a hierarchical topography.

Moths are known for their anti-reflective eyes. The anti-reflection properties of moths' eyes are based on their surface structure consisting of submicrometer protrusions ~200 nm in height and spacing. Wavelength of visible light is much larger than the size of the surface structures at the cornea, and thus the incident light does not see a sharp interface, but rather a gradual transition of the refractive index between the air and the cornea.[132-133]

3. Summary and outlook

Super liquid-repellent surfaces found in nature and those used in artificial applications need to combine at least three properties: a high apparent receding contact angle, high impalement pressure, and mechanical robustness. Depending on the specific application they also need to be optically transparent, reduce biofouling, or prevent icing. To combine these requirements hierarchical structures are needed. This explains why a broad range of different types of hierarchical superhydrophobic surfaces has evolved in nature.

Nanostructures are necessary to achieve a high apparent receding contact angle and high liquid-entry-pressure at the same time. Hierarchical surface structure can further increase the apparent receding contact angle, lower the drop adhesion to the surface and prevent impalement of impacting drops. Additionally, hierarchical surface design can be used to reduce the contact time of impacting drops. Other properties controllable by surface structures at different length scales include structural colors and anti-reflective properties of surfaces.

In the case of artificial super liquid-repellent surfaces, insufficient mechanical stability still remains the main issue limiting their large-scale use in actual applications. Enhanced mechanical robustness is one of the most important functions of a hierarchical surface design. On the large length scale, micro- and macroprotrusions can protect mechanically weak nanostructures in between without compromising the anti-wetting properties.

Condensing water on surface structures can lead to loss of superhydrophobicity under supersaturated humidity. Suitable hierarchical surface design, or one-tier nanostructures with conical geometry mimicked from cicada wings, can efficiently remove condensed water from surfaces. Combining a hierarchical surface design and conical geometry in every length scale could be the ideal structure to prevent condensation wetting.

The combination of a high apparent receding contact angle, high liquid-entry-pressure and mechanical robustness still remains a challenge. Combining these properties, even with optical transparency, anti-reflecting, anti-fouling or photocatalytic properties, is a future challenge in developing hierarchical surfaces.

References

1. Young, T., An essay on the cohesion of fluids. *Phil. Trans. R. Soc. Lond.* **1805,** *95*, 65-87.
2. Quéré, D., Wetting and Roughness. *Annu. Rev. Mater. Res.* **2008,** *38* (1), 71-99.
3. Deng, X.; Schellenberger, F.; Papadopoulos, P.; Vollmer, D.; Butt, H.-J., Liquid drops impacting superamphiphobic coatings. *Langmuir* **2013,** *29* (25), 7847-7856.

4. Papadopoulos, P.; Mammen, L.; Deng, X.; Vollmer, D.; Butt, H.-J., How superhydrophobicity breaks down. *Proc. Natl. Acad. Sci. U.S.A.* **2013,** *110* (9), 3254-3258.

5. Li, X. M.; Reinhoudt, D.; Crego-Calama, M., What do we need for a superhydrophobic surface? A review on the recent progress in the preparation of superhydrophobic surfaces. *Chem. Soc. Rev.* **2007,** *36* (8), 1350-1368.

6. Lafuma, A.; Quéré, D., Superhydrophobic states. *Nat. Mater.* **2003,** *2* (7), 457-60.

7. Teisala, H.; Geyer, F.; Haapanen, J.; Juuti, P.; Mäkelä, J. M.; Vollmer, D.; Butt, H.-J., Ultrafast processing of hierarchical nanotexture for a transparent superamphiphobic coating with extremely low roll-off angle and high impalement pressure. *Adv. Mater.* **2018,** *30*, 1706529.

8. Shirtcliffe, N. J.; McHale, G.; Newton, M. I.; Perry, C. C., Wetting and wetting transitions on copper-based super-hydrophobic surfaces. *Langmuir* **2005,** *21*, 937-943.

9. Choi, C. H.; Kim, C. J., Large slip of aqueous liquid flow over a nanoengineered superhydrophobic surface. *Phys. Rev. Lett.* **2006,** *96* (6), 066001.

10. Dorrer, C.; Rühe, J., Wetting of silicon nanograss: from superhydrophilic to superhydrophobic surfaces. *Adv. Mater.* **2008,** *20* (1), 159-163.

11. Gao, N.; Geyer, F.; Pilat, D. W.; Wooh, S.; Vollmer, D.; Butt, H.-J.; Berger, R., How drops start sliding over solid surfaces. *Nat. Phys.* **2018,** *14*, 191-196.

12. Bico, J.; Marzolin, C.; Quéré, D., Pearl drops. *Europhys. Lett.* **1999,** *47*, 220-226.

13. Fürstner, R.; Barthlott, W., Wetting and self-cleaning properties of artificial superhydrophobic surfaces. *Langmuir* **2005,** *21*, 956-961.

14. Zhao, H.; Law, K. Y., Directional self-cleaning superoleophobic surface. *Langmuir* **2012,** *28* (32), 11812-11818.

15. Schellenberger, F.; Encinas, N.; Vollmer, D.; Butt, H.-J., How water advances on superhydrophobic surfaces. *Phys. Rev. Lett.* **2016,** *116* (9), 096101.

16. Cassie, A. B. D.; Baxter, S., Wettability of porous surfaces. *Trans. Faraday Soc.* **1944,** *40*, 546-551.

17. Ma, M.; Hill, R. M., Superhydrophobic surfaces. *Curr. Opin. Colloid Interface Sci.* **2006,** *11* (4), 193-202.

18. Xia, F.; Jiang, L., Bio-inspired, smart, multiscale interfacial materials. *Adv. Mater.* **2008,** *20* (15), 2842-2858.

19. Drelich, J.; Marmur, A., Physics and applications of superhydrophobic and superhydrophilic surfaces and coatings. *Surface Innovations* **2013,** *2*, 211-227.

20. Tian, X.; Verho, T.; Ras, R. H. A., Moving superhydrophobic surfaces toward real-world applications. *Science* **2016,** *352* (6282), 142-143.

21. Xu, Q.; Zhang, W.; Dong, C.; Sreeprasad, T. S.; Xia, Z., Biomimetic self-cleaning surfaces: synthesis, mechanism and applications. *J. R. Soc. Interface* **2016,** *13*, 20160300.

22. Martin, S.; Brown, P. S.; Bhushan, B., Fabrication techniques for bioinspired, mechanically-durable, superliquiphobic surfaces for water, oil, and surfactant repellency. *Adv. Colloid Interface Sci.* **2017,** *241*, 1-23.

23. Ras, R. H. A.; Marmur, A., *Non-wettable Surfaces: Theory, Preparation and Applications*. Royal Society of Chemistry: 2017; p 391.

24. Nosonovsky, M., Multiscale roughness and stability of superhydrophobic biomimetic interfaces. *Langmuir* **2007,** *23*, 3157-3161.

25. Roach, P.; Shirtcliffe, N. J.; Newton, M. I., Progess in superhydrophobic surface development. *Soft Matter* **2008,** *4* (2), 224-240.

26. Teisala, H.; Tuominen, M.; Kuusipalo, J., Superhydrophobic coatings on cellulose-based materials: fabrication, properties, and applications. *Adv. Mater. Interfaces* **2014,** *1*, 1300026.

27. Churaev, N. V.; Starov, V. M.; Derjaguin, B. V., The shape of the transition zone between a thin film and bulk liquid and the line tension. *J. Colloid Interface Sci.* **1982,** *89* (1), 16-24.

28. Marmur, A., Hydro- hygro- oleo- omni-phobic? Terminology of wettability classification. *Soft Matter* **2012,** *8* (26), 6867.

29. Butt, H.-J.; Roisman, I. V.; Brinkmann, M.; Papadopoulos, P.; Vollmer, D.; Semprebon, C., Characterization of super liquid-repellent surfaces. *Curr. Opin. Colloid Interface Sci.* **2014,** *19* (4), 343-354.

30. Wenzel, R. N., Resistance of solid surfaces to wetting by water. *Ind. Eng. Chem.* **1936,** *28* (8), 988-994.

31. Pilat, D. W.; Papadopoulos, P.; Schaffel, D.; Vollmer, D.; Berger, R.; Butt, H.-J., Dynamic measurement of the force required to move a liquid drop on a solid surface. *Langmuir* **2012,** *28* (49), 16812-16820.

32. Koc, Y.; de Mello, A. J.; McHale, G.; Newton, M. I.; Roach, P.; Shirtcliffe, N. J., Nano-scale superhydrophobicity: suppression of protein adsorption and promotion of flow-induced detachment. *Lab Chip* **2008,** *8* (4), 582-6.

33. Cao, L.; Jones, A. K.; Sikka, V. K.; Wu, J.; Gao, D., Anti-icing superhydrophobic coatings. *Langmuir* **2009,** *25* (21), 12444-12448.

34. Mishchenko, L.; Hatton, B.; Bahadur, V.; Taylor, J. A.; Krupenkin, T.; Aizenberg, J., Design of ice-free nanostructured surfaces based on repulsion of impacting water droplets. *ACS Nano* **2010,** *4* (12), 7699-7707.

35. Paven, M.; Papadopoulos, P.; Schöttler, S.; Deng, X.; Mailänder, V.; Vollmer, D.; Butt, H.-J., Super liquid-repellent gas membranes for carbon dioxide capture and heart-lung machines. *Nat. Commun.* **2013,** *4*, 2512.

36. Geyer, F.; Schönecker, C.; Butt, H.-J.; Vollmer, D., Enhancing CO2 capture using robust superomniphobic membranes. *Adv. Mater.* **2017,** *29* (5), 1603524.

37. Zhang, J.; Seeger, S., Polyester Materials with Superwetting Silicone Nanofilaments for Oil/Water Separation and Selective Oil Absorption. *Adv. Funct. Mater.* **2011,** *21* (24), 4699-4704.

38. Calcagnile, P.; Fragouli, D.; Bayer, I. S.; Anyfantis, G. C.; Martiradonna, L.; Cozzoli, P. D.; Cingolani, R.; Athanassiou, A., Magnetically driven floating foams for the removal of oil contaminants from water. *ACS Nano* **2012,** *6* (6), 5413-5419.

39. Zhai, L.; Berg, M. C.; Cebeci, F. Ç.; Kim, Y.; Milwid, J. M.; Rubner, M. F.; Cohen, R. E., Patterned superhydrophobic surfaces: Toward a synthetic mimic of the Namib desert beetle. *Nano Lett.* **2006,** *6* (6), 1213-1217.

40. Boreyko, J. B.; Chen, C. H., Self-propelled dropwise condensate on superhydrophobic surfaces. *Phys. Rev. Lett.* **2009,** *103* (18), 184501.

41. Deng, X.; Paven, M.; Papadopoulos, P.; Ye, M.; Wu, S.; Schuster, T.; Klapper, M.; Vollmer, D.; Butt, H.-J., Solvent-free synthesis of microparticles on superamphiphobic surfaces. *Angew. Chem. Int. Ed. Engl.* **2013,** *52* (43), 11286-11289.

42. Costa, A. M. S.; Mano, J. F., Solvent-free strategy yields size and shape-uniform capsules. *J. Am. Chem. Soc.* **2017,** *139* (3), 1057-1060.

43. Wooh, S.; Huesmann, H.; Tahir, M. N.; Paven, M.; Wichmann, K.; Vollmer, D.; Tremel, W.; Papadopoulos, P.; Butt, H.-J., Synthesis of mesoporous supraparticles on superamphiphobic surfaces. *Adv. Mater.* **2015,** *27* (45), 7338-7343.

44. Wong, W. S.; Liu, G.; Tricoli, A., Superamphiphobic bionic proboscis for contamination-free manipulation of nano and core-shell droplets. *Small* **2017,** *13* (14), 1603688.

45. Balu, B.; Berry, A. D.; Hess, D. W.; Breedveld, V., Patterning of superhydrophobic paper to control the mobility of micro-liter drops for two-dimensional lab-on-paper applications. *Lab Chip* **2009,** *9* (21), 3066-3075.

46. Li, J.; Liu, X.; Ye, Y.; Zhou, H.; Chen, J., Fabrication of superhydrophobic CuO surfaces with tunable water adhesion. *J. Phys. Chem. C* **2011,** *115* (11), 4726-4729.

47. Jin, M.; Feng, X.; Feng, L.; Sun, T.; Zhai, J.; Li, T.; Jiang, L., Superhydrophobic aligned polystyrene nanotube films with high adhesive force. *Adv. Mater.* **2005,** *17* (16), 1977-1981.

48. Rahmawan, Y.; Xu, L.; Yang, S., Self-assembly of nanostructures towards transparent, superhydrophobic surfaces. *J. Mater. Chem. A* **2013,** *1* (9), 2955-2969.

49. Golovin, K.; Lee, D. H.; Mabry, J. M.; Tuteja, A., Transparent, flexible, superomniphobic surfaces with ultra-low contact angle hysteresis. *Angew. Chem. Int. Ed. Engl.* **2013,** *52* (49), 13007-13011.

50. Deng, X.; Mammen, L.; Zhao, Y.; Lellig, P.; Mullen, K.; Li, C.; Butt, H.-J.; Vollmer, D., Transparent, thermally stable and mechanically robust superhydrophobic surfaces made from porous silica capsules. *Adv. Mater.* **2011,** *23* (26), 2962-2965.

51. Extrand, C. W., Designing for optimum liquid repellency. *Langmuir* **2006,** *22*, 1711-1714.

52. Butt, H.-J.; Vollmer, D.; Papadopoulos, P., Super liquid-repellent layers: The smaller the better. *Adv. Colloid Interface Sci.* **2015,** *222*, 104-109.

53. Kota, A. K.; Kwon, G.; Tuteja, A., The design and applications of superomniphobic surfaces. *NPG Asia Mater.* **2014,** *6* (7), e109.

54. Li, W.; Amirfazli, A., Hierarchical structures for natural superhydrophobic surfaces. *Soft Matter* **2008,** *4* (3), 462-466.

55. Koch, K.; Bhushan, B.; Jung, Y. C.; Barthlott, W., Fabrication of artificial Lotus leaves and significance of hierarchical structure for superhydrophobicity and low adhesion. *Soft Matter* **2009,** *5* (7), 1386-1393.

56. Busscher, H. J.; Stokroos, I.; Golverdingen, J. G.; Schakenraad, J. M., Adhesion and spreading of human fibroblasts on superhydrophobic FEP-Teflon. *Cells Mater.* **1991,** *1* (3), 243-249.

57. Busscher, H. J.; Stokroos, I.; Van Der Mei, H. C.; Rouxhet, P. G.; Schakenraad, J. M., Preparation and characterization of superhydrophobic FEP-Teflon surfaces. *J. Adhesion Sci. Technol.* **1992,** *6* (3), 347-356.

58. Barthlott, W.; Neinhuis, C., Purity of the sacred lotus, or escape from contamination in biological surfaces. *Planta* **1997,** *202*, 1-8.

59. Wagner, T.; Neinhuis, C.; Barthlott, W., Wettability and contaminability of insect wings as a function of their surface sculptures. *Acta Zool.* **1996,** *77* (3), 213-225.

60. Feng, L.; Li, S.; Li, Y.; Li, H.; Zhang, L.; Zhai, J.; Song, Y.; Liu, B.; Jiang, L.; Zhu, D., Super-hydrophobic surfaces: From natural to artificial. *Adv. Mater.* **2002,** *14* (24), 1857-1860.

61. Otten, A.; Herminghaus, S., How plants keep dry: A physicist's point of view. *Langmuir* **2004,** *20*, 2405-2408.

62. Feng, L.; Zhang, Y.; Xi, J.; Zhu, Y.; Wang, N.; Xia, F.; Jiang, L., Petal effect: A superhydrophobic state with high adhesive force. *Langmuir* **2008,** *24*, 4114-4119.

63. Koch, K.; Bhushan, B.; Barthlott, W., Diversity of structure, morphology and wetting of plant surfaces. *Soft Matter* **2008,** *4*, 1943-1963.

64. Gao, X.; Jiang, L., Water-repellent legs of water striders. *Nature* **2004,** *432*, 36.

65. Watson, G. S.; Cribb, B. W.; Watson, J. A., How micro/nanoarchitecture facilitates anti-wetting: An elegant hierarchical design on the termite wing. *ACS Nano* **2010,** *4* (1), 129-136.

66. Cheng, Y.-T.; Rodak, D. E., Is the lotus leaf superhydrophobic? *Appl. Phys. Lett.* **2005,** *86* (14), 144101.

67. Zheng, Y.; Gao, X.; Jiang, L., Directional adhesion of superhydrophobic butterfly wings. *Soft Matter* **2007,** *3* (2), 178-182.

68. Gao, X.; Yan, X.; Yao, X.; Xu, L.; Zhang, K.; Zhang, J.; Yang, B.; Jiang, L., The dry-style antifogging properties of mosquito compound eyes and artificial analogues prepared by soft lithography. *Adv. Mater.* **2007,** *19* (17), 2213-2217.

69. Lee, W.; Jin, M.-K.; Yoo, W.-C.; Lee, J.-K., Nanostructuring of a polymeric substrate with well-defined nanometer-scale topography and tailored surface wettability. *Langmuir* **2004,** *20*, 7665-7669.

70. Teisala, H.; Tuominen, M.; Kuusipalo, J., Adhesion mechanism of water droplets on hierarchically rough superhydrophobic rose petal surface. *J. Nanomater.* **2011,** *2011*, 818707.

71. Wu, D.; Wang, J.-N.; Wu, S.-Z.; Chen, Q.-D.; Zhao, S.; Zhang, H.; Sun, H.-B.; Jiang, L., Three-level biomimetic rice-leaf surfaces with controllable anisotropic sliding. *Adv. Funct. Mater.* **2011,** *21* (15), 2927-2932.

72. Winkel, A.; Colmer, T. D.; Ismail, A. M.; Pedersen, O., Internal aeration of paddy field rice (Oryza sativa) during complete submergence - importance of light and floodwater O2. *New Phytol.* **2013,** *197* (4), 1193-1203.

73. Armstrong, W., Aeration in higher plants. *Adv. Bot. Res.* **1980,** *7*, 225-332.

74. Barthlott, W., *Scanning electron microscopy of the epidermal surface in plants, in: Scanning Electron Microscopy in Taxonomy and Functional Morphology*. The Systematics Association, Clarendon Press: Oxford, 1990; Vol. 41, p 69-83.

75. Barthlott, W., *Die Selbstreinigungsfähigkeit pflanzlicher Oberflächen durch Epicuticularwachse, in: Verantwortung für die Zukunft. Klima- und Umweltforschung an der Universität Bonn*. Bonn, 1992; p 117-120.

76. Dettre, R. H.; Johnson, R. E., Contact angle hysteresis - porous surfaces. *SCI Monograph* **1967,** *25*, 144-163.

77. Onda, T.; Shibuichi, S.; Satoh, N.; Tsujii, K., Super-water-repellent fractal surfaces. *Langmuir* **1996,** *12* (9), 2125-2127.

78. Erbil, H. Y.; Demirel, A. L.; Avci, Y.; Mert, O., Transformation of a simple plastic into a superhydrophobic surface. *Science* **2003,** *299*, 1377-1380.

79. Jin, M.; Feng, X.; Xi, J.; Zhai, J.; Cho, K.; Feng, L.; Jiang, L., Super-hydrophobic PDMS surface with ultra-low adhesive force. *Macromol. Rapid Commun.* **2005,** *26* (22), 1805-1809.

80. Zhu, L.; Xiu, Y.; Xu, J.; Tamirisa, P. A.; Hess, D. W.; Wong, C.-P., Superhydrophobicity on two-tier rough surfaces fabricated by controlled growth of aligned carbon nanotube arrays coated with fluorocarbon. *Langmuir* **2005,** *21*, 11208-11212.

81. Ming, W.; Wu, D.; van Benthem, R.; de With, G., Superhydrophobic films from raspberry-like particles. *Nano Lett.* **2005,** *5* (11), 2298-2301.

82. D'Acunzi, M.; Mammen, L.; Singh, M.; Deng, X.; Roth, M.; Auernhammer, G. K.; Butt, H.-J.; Vollmer, D., Superhydrophobic surfaces by hybrid raspberry-like particles. *Faraday Discuss.* **2010,** *146*, 35-48.

83. Bittoun, E.; Marmur, A., The role of multiscale roughness in the Lotus effect: is it essential for super-hydrophobicity? *Langmuir* **2012,** *28* (39), 13933-13942.

84. Patankar, N. A., On the modeling of hydrophobic contact angles on rough surfaces. *Langmuir* **2003,** *19*, 1249-1253.

85. Papadopoulos, P.; Vollmer, D.; Butt, H.-J., Long-term repellency of liquids by superoleophobic surfaces. *Phys. Rev. Lett.* **2016,** *117* (4), 046102.

86. Marmur, A., Wetting on hydrophobic rough surfaces: To be heterogeneous or not to be? *Langmuir* **2003,** *19*, 8343-8348.

87. Patankar, N. A., Transition between superhydrophobic states on rough surfaces. *Langmuir* **2004,** *20*, 7097-7102.

88. Patankar, N. A., Mimicking the lotus effect: influence of double roughness structures and slender pillars. *Langmuir* **2004,** *20*, 8209-8213.

89. Su, Y.; Ji, B.; Zhang, K.; Gao, H.; Huang, Y.; Hwang, K., Nano to micro structural hierarchy is crucial for stable superhydrophobic and water-repellent surfaces. *Langmuir* **2010,** *26* (7), 4984-4989.

90. Liu, T.; Sun, W.; Sun, X.; Ai, H., Thermodynamic analysis of the effect of the hierarchical architecture of a superhydrophobic surface on a condensed drop state. *Langmuir* **2010,** *26* (18), 14835-14841.

91. de Gennes, P.-G.; Brochard-Wyart, F.; Quéré, D., *Capillarity and Wetting Phenomena: Drops, Bubbles, Pearls, Waves*. Springer: New York, 2004; p 292.

92. Deng, T.; Varanasi, K. K.; Hsu, M.; Bhate, N.; Keimel, C.; Stein, J.; Blohm, M., Nonwetting of impinging droplets on textured surfaces. *Appl. Phys. Lett.* **2009,** *94* (13), 133109.

93. Bartolo, D.; Bouamrirene, F.; Verneuil, É.; Buguin, A.; Silberzan, P.; Moulinet, S., Bouncing or sticky droplets: Impalement transitions on superhydrophobic micropatterned surfaces. *Europhys. Lett.* **2006,** *74* (2), 299-305.

94. Prakash, S.; Xi, E.; Patel, A. J., Spontaneous recovery of superhydrophobicity on nanotextured surfaces. *Proc. Natl. Acad. Sci. U.S.A.* **2016,** *113* (20), 5508-5513.

95. Zhang, B.; Chen, X.; Dobnikar, J.; Wang, Z.; Zhang, X., Spontaneous Wenzel to Cassie dewetting transition on structured surfaces. *Phys. Rev. Fluids* **2016,** *1* (7), 073904.

96. Lisi, E.; Amabili, M.; Meloni, S.; Giacomello, A.; Casciola, C. M., Self-recovery superhydrophobic surfaces: modular design. *ACS Nano* **2018,** *12* (1), 359-367.

97. Liu, Y.; Moevius, L.; Xu, X.; Qian, T.; Yeomans, J. M.; Wang, Z., Pancake bouncing on superhydrophobic surfaces. *Nat. Phys.* **2014,** *10* (7), 515-519.

98. Verho, T.; Korhonen, J. T.; Sainiemi, L.; Jokinen, V.; Bower, C.; Franze, K.; Franssila, S.; Andrew, P.; Ikkala, O.; Ras, R. H. A., Reversible switching between superhydrophobic states on a hierarchically structured surface. *Proc. Natl. Acad. Sci. U.S.A.* **2012,** *109* (26), 10210-10213.

99. Tsujii, K.; Yamamoto, T.; Onda, T.; Shibuichi, S., Super oil-repellent surfaces. *Angew. Chem. Int. Ed. Engl.* **1997,** *36* (9), 1011-1012.

100. Herminghaus, S., Roughness-induced non-wetting. *Europhys. Lett.* **2000,** *52* (2), 165-170.

101. Tuteja, A.; Choi, W.; Ma, M.; Mabry, J. M.; Mazzella, S. A.; Rutledge, G. C.; McKinley, G. H.; Cohen, R. E., Designing superoleophobic surfaces. *Science* **2007,** *318* (5856), 1618-1622.

102. Butt, H.-J.; Semprebon, C.; Papadopoulos, P.; Vollmer, D.; Brinkmann, M.; Ciccotti, M., Design principles for superamphiphobic surfaces. *Soft Matter* **2013,** *9* (2), 418-428.

103. Ye, M.; Deng, X.; Ally, J.; Papadopoulos, P.; Schellenberger, F.; Vollmer, D.; Kappl, M.; Butt, H.-J., Superamphiphobic particles: How small can we go? *Phys. Rev. Lett.* **2014,** *112* (1), 016101.

104. Zhang, B.; Zhang, X., Elucidating nonwetting of re-entrant surfaces with impinging droplets. *Langmuir* **2015,** *31* (34), 9448-9457.

105. Liu, T.; Kim, C.-J., Turning a surface superrepellent even to completely wetting liquids. *Science* **2014,** *346* (6213), 1096-1100.

106. Chu, Z.; Seeger, S., Superamphiphobic surfaces. *Chem. Soc. Rev.* **2014,** *43* (8), 2784-2798.

107. Deng, X.; Mammen, L.; Butt, H.-J.; Vollmer, D., Candle soot as a template for a transparent robust superamphiphobic coating. *Science* **2012,** *335* (6064), 67-70.

108. Fujii, T.; Sato, H.; Tsuji, E.; Aoki, Y.; Habazaki, H., Important role of nanopore morphology in superoleophobic hierarchical surfaces. *J. Phys. Chem. C* **2012,** *116* (44), 23308-23314.

109. Barthwal, S.; Kim, Y. S.; Lim, S.-H., Mechanically robust superamphiphobic aluminum surface with nanopore-embedded microtexture. *Langmuir* **2013,** *29* (38), 11966-11974.

110. Verho, T.; Bower, C.; Andrew, P.; Franssila, S.; Ikkala, O.; Ras, R. H. A., Mechanically durable superhydrophobic surfaces. *Adv. Mater.* **2011,** *23* (5), 673-678.

111. Groten, J.; Rühe, J., Surfaces with combined microscale and nanoscale structures: a route to mechanically stable superhydrophobic surfaces? *Langmuir* **2013,** *29* (11), 3765-3772.

112. Xiu, Y.; Liu, Y.; Hess, D. W.; Wong, C. P., Mechanically robust superhydrophobicity on hierarchically structured Si surfaces. *Nanotechnology* **2010,** *21* (15), 155705.

113. Zhou, H.; Wang, H.; Niu, H.; Gestos, A.; Wang, X.; Lin, T., Fluoroalkyl silane modified silicone rubber/nanoparticle composite: a super durable, robust superhydrophobic fabric coating. *Adv. Mater.* **2012,** *24* (18), 2409-2412.

114. Zimmermann, J.; Reifler, F. A.; Fortunato, G.; Gerhardt, L.-C.; Seeger, S., A simple, one-step approach to durable and robust superhydrophobic textiles. *Adv. Funct. Mater.* **2008,** *18* (22), 3662-3669.

115. Butt, H.-J.; Gao, N.; Papadopoulos, P.; Steffen, W.; Kappl, M.; Berger, R., Energy dissipation of moving drops on superhydrophobic and superoleophobic surfaces. *Langmuir* **2017,** *33* (1), 107-116.

116. Miljkovic, N.; Enright, R.; Nam, Y.; Lopez, K.; Dou, N.; Sack, J.; Wang, E. N., Jumping-droplet-enhanced condensation on scalable superhydrophobic nanostructured surfaces. *Nano Lett.* **2013,** *13* (1), 179-187.

117. Reyssat, M.; Pépin, A.; Marty, F.; Chen, Y.; Quéré, D., Bouncing transitions on microtextured materials. *Europhys. Lett.* **2006,** *74* (2), 306-312.

118. Bird, R. B.; Stewart, W. E.; Lightfoot, E. N., *Transport phenomena*. Wiley: New York, 1960; p 780.

119. Bird, J. C.; Dhiman, R.; Kwon, H. M.; Varanasi, K. K., Reducing the contact time of a bouncing drop. *Nature* **2013,** *503* (7476), 385-388.

120. Gauthier, A.; Symon, S.; Clanet, C.; Quéré, D., Water impacting on superhydrophobic macrotextures. *Nat. Commun.* **2015,** *6*, 8001.

121. Guo, C.; Zhao, D.; Sun, Y.; Wang, M.; Liu, Y., Droplet impact on anisotropic superhydrophobic surfaces. *Langmuir* **2018,** *34* (11), 3533-3540.

122. Mertaniemi, H.; Jokinen, V.; Sainiemi, L.; Franssila, S.; Marmur, A.; Ikkala, O.; Ras, R. H. A., Superhydrophobic tracks for low-friction, guided transport of water droplets. *Adv. Mater.* **2011,** *23* (26), 2911-2914.

123. Chen, C.-H.; Cai, Q.; Tsai, C.; Chen, C.-L.; Xiong, G.; Yu, Y.; Ren, Z., Dropwise condensation on superhydrophobic surfaces with two-tier roughness. *Appl. Phys. Lett.* **2007,** *90* (17), 173108.

124. Rykaczewski, K.; Paxson, A. T.; Anand, S.; Chen, X.; Wang, Z.; Varanasi, K. K., Multimode multidrop serial coalescence effects during condensation on hierarchical superhydrophobic surfaces. *Langmuir* **2013,** *29* (3), 881-891.

125. Chen, X.; Wu, J.; Ma, R.; Hua, M.; Koratkar, N.; Yao, S.; Wang, Z., Nanograssed micropyramidal architectures for continuous dropwise condensation. *Adv. Funct. Mater.* **2011,** *21* (24), 4617-4623.

126. Mouterde, T.; Lehoucq, G.; Xavier, S.; Checco, A.; Black, C. T.; Rahman, A.; Midavaine, T.; Clanet, C.; Quéré, D., Antifogging abilities of model nanotextures. *Nat. Mater.* **2017,** *16* (6), 658-663.

127. Rose, J. W., Dropwise condensation theory and experiment: a review. *Proc. Inst. Mech. Eng., A: J. Power Energy* **2002,** *216*, 115-128.

128. Boreyko, J. B.; Collier, C. P., Delayed frost growth on jumping-drop superhydrophobic surfaces. *ACS Nano* **2013,** *7* (2), 1618-1627.

129. Feng, L.; Zhang, Z.; Mai, Z.; Ma, Y.; Liu, B.; Jiang, L.; Zhu, D., A super-hydrophobic and super-oleophilic coating mesh film for the separation of oil and water. *Angew. Chem. Int. Ed. Engl.* **2004,** *43* (15), 2012-2014.

130. Mason, C. W., Structural colors in feathers I. *J. Phys. Chem.* **1923,** *27* (3), 201-251.

131. Wang, Z.; Guo, Z., Biomimetic superwettable materials with structural colours. *Chem. Commun.* **2017,** *53* (97), 12990-13011.

132. Bernhard, C. G., Structural and functional adaptation in a visual system. *Endeavour* **1967,** *26* (98), 79.

133. Clapham, P. B.; Hutley, M. C., Reduction of lens reflexion by the "moth eye" principle. *Nature* **1973,** *244*, 281-282.

Acknowledgements

This work was funded by the ERC advanced grant 340391 – SUPRO and the Collaborative Research Center 1194. H.T. gratefully acknowledges the Alexander von Humboldt Foundation for financial support.

Table of Contents Graphic

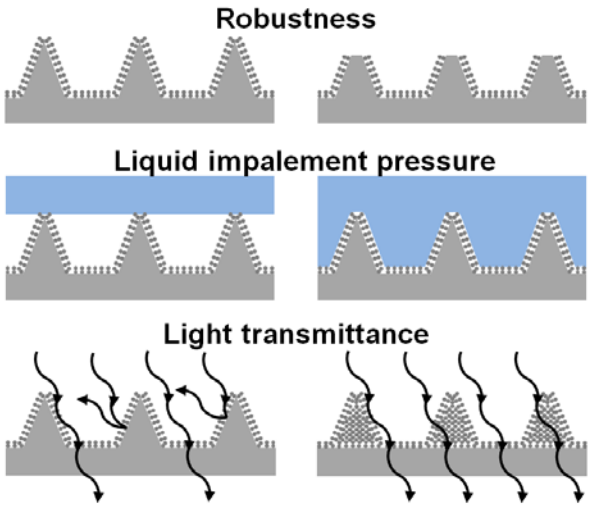

Authors' biographies

Hannu Teisala studied Materials Science at Tampere University of Technology in Finland. He received his M.Sc. in Paper Converting and Packaging Technology in 2009 and defended his thesis on liquid flame sprayed superhydrophobic functional nanoparticle coatings on cellulose-based materials in November 2013. After working for two years as a postdoctoral researcher and project manager in Tampere, he joined the group of Prof. Hans-Jürgen Butt and Prof. Doris Vollmer in Mainz in 2015 to investigate liquid-infused slippery surfaces. His main research interests include wetting, super liquid-repellent, slippery and ice-repellent surfaces, photocatalysis, and micro-/nanostructured surfaces and coatings.

Hans-Jürgen Butt studied physics in Hamburg and Göttingen, Germany. Then he went to the Max Planck Institute of Biophysics in Frankfurt. After receiving his Ph.D. in 1989 he went as a postdoctoral researcher to Santa Barbara, California, where he used the newly developed atomic force microscope. From 1990-95 he worked as a researcher back in Germany at the Max Planck Institute for Biophysics. In 1996 he became associate professor for physical chemistry at the University of Mainz, four years later full professor at the University of Siegen. In 2002 he joined the Max Planck Institute for Polymer Research in Mainz and became director for experimental physics of interfaces.